

UNCLASSIFIED

AD 282 651

*Reproduced
by the*

**ARMED SERVICES TECHNICAL INFORMATION AGENCY
ARLINGTON HALL STATION
ARLINGTON 12, VIRGINIA**



UNCLASSIFIED

NOTICE: When government or other drawings, specifications or other data are used for any purpose other than in connection with a definitely related government procurement operation, the U. S. Government thereby incurs no responsibility, nor any obligation whatsoever; and the fact that the Government may have formulated, furnished, or in any way supplied the said drawings, specifications, or other data is not to be regarded by implication or otherwise as in any manner licensing the holder or any other person or corporation, or conveying any rights or permission to manufacture, use or sell any patented invention that may in any way be related thereto.

62-4-5

282651

ARL 62-387

HYPERSONIC VISCOUS FLOW OVER CONES
AT NOMINAL MACH 11 IN AIR

CATALOGED BY ASTIA
AS AD No.

JOHN D. ANDERSON, JR., 1/LT., USAF
HYPERSONIC RESEARCH LABORATORY

JULY 1962

AERONAUTICAL RESEARCH LABORATORIES
OFFICE OF AEROSPACE RESEARCH
UNITED STATES AIR FORCE

282 651

ASTIA
RECEIVED
AUG 27 1962
TISIA A



FOR ERRATA

AD 282 651

THE FOLLOWING PAGES ARE CHANGES

TO BASIC DOCUMENT

AD 282651

ERRATA - March 1963

The following corrections are applicable to ARL 62-387, entitled "Hypersonic Viscous Flow Over Cones At Nominal Mach 11 In Air", dated July 1962.

Page 17, line 17 should read:

$$\frac{d \delta^*}{dx} = \frac{1.74}{2} \sqrt{\frac{C}{Re_{2x}}} \left\{ \frac{\pi}{2} \left[\frac{T_w}{T_2} - \frac{\sigma(\gamma-1)}{4} M_2^2 \right] - \left[1 + \sigma^{1/3} \left(\frac{T_w}{T_2} - \frac{T_{aw}}{T_2} \right) \right] \right\}$$

The above changes had the following effect on all analytical curves obtained by Talbot's method:

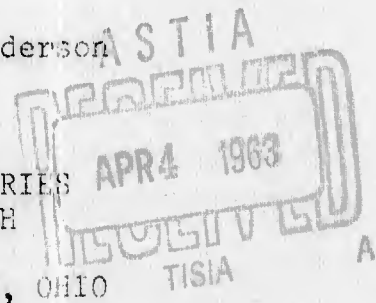
- (a) The computed values for induced pressure increment for the 5° cone should be increased 5%.
- (b) The computed values for induced pressure increment for the 10° cone should be increased 6%.
- (c) The computed values for induced pressure increment for the 15° cone should be decreased 5%.
- (d) The computed values for induced pressure increment for the 20° cone should be decreased 14%.

All other curves, both analytical and experimental, are correct.

All the above changes had no effect on the general conclusions made in the subject report, and they should not be altered.

John D. Anderson

AERONAUTICAL RESEARCH LABORATORIES
 OFFICE OF AEROSPACE RESEARCH
 UNITED STATES AIR FORCE
 WRIGHT-PATTERSON AIR FORCE BASE, OHIO



NOTICES

When Government drawings, specifications, or other data are used for any purpose other than in connection with a definitely related Government procurement operation, the United States Government thereby incurs no responsibility nor any obligation whatsoever; and the fact that the Government may have formulated, furnished, or in any way supplied the said drawings, specifications, or other data, is not to be regarded by implication or otherwise as in any manner licensing the holder or any other person or corporation, or conveying any rights or permission to manufacture, use, or sell any patented invention that may in any way be related thereto.

- - - - -

Qualified requesters may obtain copies of this report from the Armed Services Technical Information Agency, (ASTIA), Arlington Hall Station, Arlington 12, Virginia.

- - - - -

This report has been released to the Office of Technical Services, U. S. Department of Commerce, Washington 25, D. C. for sale to the general public.

- - - - -

Copies of ARL Technical Documentary Reports should not be returned to Aeronautical Research Laboratory unless return is required by security considerations, contractual obligations, or notices on a specific document.

ARL 62-387

HYPersonic VISCOUS FLOW OVER CONES
AT NOMINAL MACH 11 IN AIR

JOHN D. ANDERSON JR., 1/LT., USAF

HYPersonic RESEARCH LABORATORY

JULY 1962

PROJECT 7064
TASK 7064-01

AERONAUTICAL RESEARCH LABORATORIES
OFFICE OF AEROSPACE RESEARCH
UNITED STATES AIR FORCE
WRIGHT-PATTERSON AIR FORCE BASE, OHIO

FOREWORD

This report covers a limited investigation of self-induced pressures on cones in hypersonic flow. The investigation was an in-house study performed within the Hypersonic Research Laboratory of the Aeronautical Research Laboratories, Office of Aerospace Research, United States Air Force. The work was limited in order to complete the report prior to the author's departure from the Laboratory and release from the U.S.A.F. and was performed under Task 7064-01.

The author wishes to acknowledge Col. Andrew Boreske, Jr., Hypersonic Research Laboratory Chief, for making available the funds and facility utilized for this investigation and to Capt. Walter W. Wells also of the Hypersonic Research Laboratory for his assistance with some numerical analyses performed during the study.

ABSTRACT

Experimental results were obtained on weak-interaction, self-induced pressures on cones at nominal Mach 11 in air using the ARL 3-inch continuous flow hypersonic wind tunnel. The results at zero angle of attack were compared with Probstein's first-order weak-interaction theory and with Talbot's numerical method for predicting self-induced pressures. Theory agreed well with the experimental data for 5-degree and 10-degree semivertex angle cones, but over-estimated the experimental induced pressures for 15-degree and 20-degree cones. The results were correlated reasonably well by the hypersonic viscous-interaction parameter and the hypersonic similarity parameter. The experimental results obtained for the 10-, 15-, and 20-degree cones at angles of attack from -15 to 15 degrees compared favorably with Newtonian theory for angles of attack greater than 3 degrees. For values less than 3 degrees, Newtonian theory did not agree with the experimental results.

TABLE OF CONTENTS

| | Page |
|--------------------------------------|------|
| INTRODUCTION | 1 |
| APPARATUS. | 5 |
| TEST PROCEDURE AND RESULTS | 7 |
| DISCUSSION | 10 |
| CONCLUSIONS. | 12 |
| REFERENCES | 14 |
| APPENDIX A | 16 |
| APPENDIX B | 17 |
| APPENDIX C | 19 |

LIST OF ILLUSTRATIONS

| <u>Figure</u> | | <u>Page</u> |
|---------------|---|-------------|
| 1 | Schematic of flow over cone | 20 |
| 2 | ARL 3-Inch Hypersonic Wind Tunnel | 21 |
| 3 | 5-Degree and 10-Degree Semivertex Angle Cone Models | 22 |
| 4 | 15-Degree and 20-Degree Semivertex Angle Cone Models | 23 |
| 5 | 5-Degree Model in Tunnel Test Section | 24 |
| 6 | Inclined Silicone Oil Manometer | 25 |
| 7 | Induced Pressure Increment vs. x , $\Theta_c = 5^\circ$, $M = 10.72$ | 26 |
| 8 | Induced Pressure Increment vs. x , $\Theta_c = 10^\circ$, $M = 10.72$ | 27 |
| 9 | Induced Pressure Increment vs. x , $\Theta_c = 10^\circ$, $M = 10.86$ | 28 |
| 10 | Induced Pressure Increment vs. x , $\Theta_c = 10^\circ$, $M = 10.95$ | 29 |
| 11 | Induced Pressure Increment vs. x , $\Theta_c = 15^\circ$, $M = 10.72$ | 30 |
| 12 | Induced Pressure Increment vs. x , $\Theta_c = 15^\circ$, $M = 10.86$ | 31 |
| 13 | Induced Pressure Increment vs. x , $\Theta_c = 15^\circ$, $M = 10.95$ | 32 |
| 14 | Induced Pressure Increment vs. x , $\Theta_c = 20^\circ$, $M = 10.72$ | 33 |
| 15 | Induced Pressure Increment vs. x , $\Theta_c = 20^\circ$, $M = 10.86$ | 34 |
| 16 | Induced Pressure Increment vs. x , $\Theta_c = 20^\circ$, $M = 10.95$ | 35 |
| 17 | Induced Pressure Increment vs. $\bar{\chi}_c$, $\Theta_c = 5^\circ$ | 36 |
| 18 | Induced Pressure Increment vs. $\bar{\chi}_c$, $\Theta_c = 10^\circ$ | 37 |
| 19 | Induced Pressure Increment vs. $\bar{\chi}_c$, $\Theta_c = 15^\circ$ | 38 |
| 20 | Induced Pressure Increment vs. $\bar{\chi}_c$, $\Theta_c = 20^\circ$ | 39 |
| 21 | * Pressure Coefficient vs. α , $\Theta_c = 10^\circ$, $M = 10.72$ | 40 |
| 22 | Pressure Coefficient vs. α , $\Theta_c = 10^\circ$, $M = 10.86$ | 41 |
| 23 | Pressure Coefficient vs. α , $\Theta_c = 10^\circ$, $M = 10.95$ | 42 |

LIST OF ILLUSTRATIONS (CONT'D)

| <u>Figure</u> | | <u>Page</u> |
|---------------|---|-------------|
| 24 | Pressure Coefficient vs. α , $\Theta_c = 15^\circ$, $M = 10.72$ | 43 |
| 25 | Pressure Coefficient vs. α , $\Theta_c = 15^\circ$, $M = 10.86$ | 44 |
| 26 | Pressure Coefficient vs. α , $\Theta_c = 15^\circ$, $M = 10.95$ | 45 |
| 27 | Pressure Coefficient vs. α , $\Theta_c = 20^\circ$, $M = 10.72$ | 46 |
| 28 | Pressure Coefficient vs. α , $\Theta_c = 20^\circ$, $M = 10.86$ | 47 |
| 29 | Pressure Coefficient vs. α , $\Theta_c = 20^\circ$, $M = 10.95$ | 48 |

LIST OF SYMBOLS

| | |
|-------------|--|
| c_p | Specific heat at constant pressure |
| c_v | Specific heat at constant volume |
| C_p | Pressure coefficient = $\frac{P - P_\infty}{\frac{1}{2} \rho_\infty V_\infty^2} = \frac{2}{\gamma M_\infty^2} \left(\frac{P}{P_\infty} - 1 \right)$ |
| C | Constant defined by the linear relationship: $C = \frac{\mu_w / \mu_c}{T_w / T_c}$ |
| k | Hypersonic similarity parameter = $\Theta_c M_\infty$ |
| M_∞ | Free-stream Mach number |
| M_c | Inviscid Mach number on cone surface |
| P | Measured pressure from experiment |
| P_c | Inviscid pressure on cone surface |
| P_2 | Pressure at edge of boundary layer |
| P_0 | Wind tunnel reservoir stagnation pressure |
| P_∞ | Free-stream static pressure |
| Re_∞ | Free-stream Reynolds number per foot |
| Re_{cx} | Reynolds number on cone surface based on inviscid conditions and distance along the cone surface from the tip |
| T_∞ | Free-stream temperature |
| T_2 | Temperature at outer edge of boundary layer |
| T_w | Measured temperature of model surface |
| T_0 | Wind tunnel reservoir stagnation temperature |
| T_c | Inviscid temperature at cone surface |
| V_∞ | Free-stream velocity |
| X | Distance along the cone surface from the tip |
| α | Angle of attack |
| γ | Ratio of specific heats = c_p / c_v |
| δ^* | Displacement thickness of the boundary layer |
| Θ_c | Cone semivertex angle |

LIST OF SYMBOLS (CONT'D)

$$\Theta_\delta \quad \text{Tan}^{-1} \frac{d\delta^*}{dx}$$

$$\Theta_2 \quad \Theta_c + \Theta_\delta$$

μ_∞ Coefficient of viscosity in free-stream at temperature T_∞

μ_c Coefficient of viscosity at temperature T_c

μ_w Coefficient of viscosity on model surface at temperature T_w

ρ_∞ Free-stream density

$\bar{\chi}_c$ Hypersonic interaction parameter = $M_c^3 \sqrt{\frac{C}{Re_{cx}}}$

INTRODUCTION

Within the general field of aerodynamics, the past decade has witnessed a considerable concentration of study and experimental research on the high-speed regime known as hypersonic flow. This regime encompasses such high-speed characteristics as large temperature gradients through shock waves and boundary layers, closeness of shock waves to body surfaces, and the considerable influence of boundary layers on the external inviscid flow. The subject of this report is a study of only one of the many phenomena that are characteristic of hypersonic flow, namely, the effect of self-induced (or boundary layer induced) interactions on surface pressure.

SELF-INDUCED PRESSURES

Cones are the object of study for this report, and the analytical model of the flow over a cone is shown in Figure 1. Due to the large temperature difference across a hypersonic boundary layer, the displacement thickness becomes relatively large, and in this case the displacement thickness adds to the cone surface such that the effective shape is an ogive. The angular direction of the inviscid flow at the edge of the boundary layer is the sum of the cone angle, Θ_c , and the angle, Θ_s , defined by the slope of the displacement thickness distribution, $\Theta_s = \tan^{-1} \frac{d\delta^*}{dx}$. This outward displacement of the inviscid flow causes a higher pressure on the cone surface than would be predicted by the exact Taylor-Maccoll cone theory, and also causes a pressure gradient along the cone surface. These pressures, hereafter called self-induced pressures, also in turn effect the rate of growth of the boundary layer, and this dependence of the boundary layer growth on the self-induced pressures (which are not known in advance) constitutes the fundamental analytical problem for predicting pressures influenced by self-induced interactions. For a more detailed description of this problem

and for an excellent discussion of viscous interactions in general, the reader should consult Reference 1.

The formulation of theory and analysis for the accurate prediction of self-induced pressures is a necessary prerequisite to the analysis of heat transfer results in hypersonic flow. In addition, the self-induced pressures must be taken into consideration for the prediction of aerodynamic forces and moments.

REVIEW OF SOME EXISTING THEORIES

At the present time, two methods of analysis are foremost in the prediction of self-induced pressures on cones in the weak interaction region. One method is based on theory formulated by Probstein (Ref 2) for the interacting flow over a cone, assuming a laminar boundary layer. This assumption is generally good for hypersonic flow over slender bodies. Essentially, Probstein set forth an analytic representation of the external inviscid flow by expressing the self-induced pressure as a Taylor Series in powers of $\frac{d\delta^*}{dx}$. After suitable treatment of this expression, Probstein achieved a compact, analytical form for the self-induced pressure as a function only of the hypersonic interaction parameter, $\bar{X} = M \sqrt{\frac{c}{R_e}}$, and the hypersonic similarity parameter, $K = M_o \theta_c$. A more detailed discussion of Probstein's theory is given in Appendix A.

Another method for predicting self-induced pressures on a cone was advanced by Talbot et al (Ref 3) (Hereafter, this method will be referred to as Talbot's method for brevity.) Essentially, the nature of Talbot's method is numerical-graphical, and the tangent cone method is employed to calculate the pressure at the edge of the boundary layer. The interdependence between induced pressure and boundary layer thickness is accounted for by a clever operation with the graphs. A more detailed discussion of Talbot's method is given in Appendix B.

Some experimental results on cone pressures at moderate angles of attack are also presented in this report, and Newtonian theory is used for a comparison. Even though Newtonian theory is not based on the viscous interaction principle, it is generally acknowledged to be useful for predicting pressure coefficients at hypersonic speeds, with increasing accuracy for high Mach numbers. Newtonian impact theory is postulated on the basis that a fluid on impact with a surface loses all its normal momentum, but none of its tangential momentum. The results show that the pressure coefficient can be expressed

$$C_p = 2 \sin^2 \phi$$

where ϕ is the angle between a tangent to the surface and the free-stream velocity vector. In many cases, observers have found that Newtonian theory compares well with empirical results when the coefficient is modified for conditions behind a normal shock. Modified Newtonian theory can be expressed

$$C_p = C_{pmax} \sin^2 \phi$$

where C_{pmax} is the pressure coefficient based on the stagnation pressure behind a normal shock. A thorough and interesting treatment of Newtonian theory for bodies of revolution can be found in Ref 4.

REVIEW OF SOME PREVIOUS EXPERIMENTAL RESULTS

A reasonable amount of data concerning pressure measurements on cones in high-speed flow is available, but in general, the data was obtained either at relatively low Mach number (compared to hypersonic) and/or at high Reynolds number. Under these conditions, the self-induced pressure effect is slight (often negligible), and the general conclusion was that cone pressures could best be predicted by inviscid exact cone theory. Representative data obtained under these conditions are reported in Refs 5 through 8.

However, some experimental results on cone pressures have been obtained under flow conditions where the induced pressure effect was sizable. Some early data was reported by Baldwin (Ref 9) at Mach 5.8 and over a range of $0.1 < \bar{\chi}_c < 1.6$.

(The hypersonic interaction parameter, $\bar{\chi}_c$, provides a good indication of the strength of viscous interactions, with higher values indicating stronger self-induced pressures. The weak-interaction region is characterized by values of $\bar{\chi}_c < 5$.) Baldwin found that his cone pressures were above the predicted values based on Probstein's first-order weak-interaction theory, but he also noted that some of the results might have been effected by the relative cone-tip bluntness.

Also, Erickson (Ref 10) observed cone pressures from Mach 16 to 18 in helium flow, and over the range $0.35 < \bar{\chi}_c < 1.5$. Obtaining his results in the small scale NASA helium tunnel (nozzle exit diameter approximately one inch), Erickson found that his pressures were considerably below the values predicted by second-order weak-interaction theory. Also, he noted the trend that, for given free-stream conditions, the self-induced pressure effect decreased as cone angle increased.

Another study of self-induced pressures on cones was made by Talbot, Koga, and Sherman (Ref 3). Pressures were measured on a 3-degree semivertex angle cone over the range $3.7 < M_\infty < 5.8$ and $0.5 < \bar{\chi}_c < 2.3$. In addition, this study also formulated the numerical-graphical method mentioned earlier for predicting self-induced pressures. Talbot's results indicated that the data could be correlated reasonably well by $\bar{\chi}_c$. Also, his results fell considerably below Probstein's second-order theory, somewhat below Probstein's first-order theory, but very close to the values predicted by his numerical-graphical method. The results of Talbot et al were obtained under favorable flow conditions for induced pressures, and the study gave some clear indications of the trends of empirical data relative to theoretical values.

CONTENT OF THE PRESENT STUDY

The purpose of the results presented in this report is to extend the range of empirical data on self-induced pressures, and to provide a comparison with existing theories in order to establish ranges of applicability. The experimental

results fall into two categories. The emphasis is placed on cone pressures at zero angle of attack, and results are given for cones with semivertex angles of 5, 10, 15, and 20 degrees over a range of $10.72 \leq M_\infty \leq 10.95$ and $0.69 \leq \bar{X}_c \leq 5.5$. In the second category are pressure coefficients on 10-, 15-, and 20-degree cones through an angle of attack range of +15 degrees to -15 degrees. The empirical results at zero angle of attack are compared with Probstein's first-order theory and Talbot's method for predicting self-induced pressures; the empirical results at angle of attack are compared with Newtonian impact and modified theories.

APPARATUS

The following is a brief discussion of the primary apparatus used to conduct the experiments and record the data.

ARL 3-INCH HYPERSONIC WIND TUNNEL

The outside configuration of the wind tunnel can be seen in Figure 2. It is an axisymmetric, continuous flow, open jet facility, using heated air as the working fluid. Air can be supplied to the stagnation chamber at any pressure between 0-3000 psi and is exhausted into a vacuum sphere which is normally maintained at 0.1 psia during operation of the tunnel. The air is heated electrically to approximately 2250°R, and the Mach number range is from 8 to better than 14. The nozzles are conical and have 3-inch exit diameters. The useful hypersonic core is slightly above one inch in diameter and the Mach number gradient along the tunnel center-line is approximately 0.40 per inch at Mach 11.

CONE MODELS

Figure 3 shows the 5- and 10-degree cone wind tunnel models, and Figure 4 shows the 15- and 20-degree cone models. Each model is made from 303 stainless steel and has a 3/8-inch base diameter with the exception of the 10-degree cone which has a base diameter of 1/2 inch. Each model has three 0.047-inch orifices in the

conical section except the 20-degree cone which has two orifices. In addition, one orifice is placed on the cylindrical portion and one in the base for each model. Chromel-Alumel thermocouples are also installed to measure surface temperature, one on the conical section and one on the cylindrical section of each model. The angle of attack of the models is controlled from outside the tunnel by a mechanical pitching mechanism. A close-up of the 5-degree cone model mounted in the test section is shown in Figure 5.

INSTRUMENTATION

The model surface pressures are measured by a multiple tube manometer inclined at 30 degrees from the horizontal and using 10-centistoke Dow Corning "200" silicone oil. Reference pressure for the manometer is maintained at approximately 0.005 mm Hg by a vacuum pump and measured by a McLeod gage. The manometer layout is shown in Figure 6.

Surface temperature on the models is measured by chromel-alumel thermocouples which are connected to a multiple channel, self-balancing, recording potentiometer.

The following is a table of reading accuracies for the primary instruments used throughout the experiments.

TABLE I

| Instrument | Range of measurement during the experiments | Reading accuracy |
|---|---|------------------------------|
| Manometer inclined at 30° from horizontal | 11 to 206 mm Si (inclined at 30°) | ±0.5 mm Si (inclined at 30°) |
| Tunnel stagnation pressure gage | 250 to 500 psia | ±1 psi |
| Tunnel stagnation temperature recorder | 520 - 2210°R | ±2.5° |
| Model pitching mechanism | -15° to 15° | ±0.1° |
| Model temperature recorder | 1170 to 1425°R | ±2.5° |

TEST PROCEDURE AND RESULTS

All experiments were conducted in the ARL 3-inch Hypersonic Wind Tunnel through a range of $10.72 \leq M_\infty \leq 10.95$. This slight variation in Mach number was due to Reynolds number effect in a fixed geometry nozzle for different stagnation conditions. The test section free stream was calibrated in detail for variation of Mach number, static temperature, and static pressure, and flow angularity was measured within the locale of the cone models. This flow angularity was used to determine the effective angle of attack for the cones.

Four cone models were utilized for studying the self-induced pressure effect. Surface pressures were measured on a 5-degree semivertex angle cone at zero angle of attack at Mach 10.72 and $Re_\infty = 1.88 \times 10^5$ per foot. The results are shown in Figures 7 and 17. Figure 7 shows the induced pressure increment, $\frac{p - p_c}{p_c}$, plotted against distance along the cone surface from the vertex. Note that p is the measured pressure and p_c is the exact inviscid cone pressure obtained from Ref 11. Figure 17 shows the induced pressure increment correlated against the hypersonic interaction parameter, $\bar{\chi}_c$.

Also, surface pressures were measured on 10-degree, 15-degree, and 20-degree semivertex angle cones at zero angle of attack at three different Mach and Reynolds number combinations: $M_\infty = 10.72$, $Re_\infty = 1.88 \times 10^5$; $M_\infty = 10.86$, $Re_\infty = 2.86 \times 10^5$; $M_\infty = 10.95$, $Re_\infty = 3.58 \times 10^5$.

The results are shown in Figures 8 through 16 where the induced pressure increment is plotted against distance along the cone, and in Figures 18 through 20 where $\frac{p - p_c}{p_c}$ is correlated against $\bar{\chi}_c$.

It should be noted that no attempts were made to insulate the cones, and therefore, nonadiabatic conditions existed on all the cones employed during the experiments.

In addition, pressures were measured on the 10-degree, 15-degree, and 20-degree semivertex angle cones pitched through a moderate angle of attack range from -15 degrees to +15 degrees at the same three Mach and Reynolds number combinations. The pressures were measured along a ray in the plane of symmetry of the flow. The results are shown in Figures 21 through 29 where the pressure coefficients are plotted against angle of attack.

DATA REDUCTION METHODS

The flow in the test section of the ARL 3-inch tunnel is conical with a positive longitudinal Mach number gradient. Therefore, the question naturally occurs about what methods are available for reducing data obtained in the conical field such that they will correlate with similar data obtained in a uniform flow field. This problem is discussed as a secondary topic in Ref 12.

In the case of the empirical data presented in this paper, two methods of data reduction were used. The first method was to form the ratio of the measured pressure to the local free-stream static pressure (the static pressure at a point in the free stream where the model pressure orifice is located). This method has been the one most commonly used by investigators faced with the conical field problem. The second method is one recently proposed in Ref 12 and will hereafter be called the Baradell-Bertram method. This method suggests a correction to the conical field data so that the results can be adjusted to a uniform field. The Baradell-Bertram method is discussed in Appendix C, and data points reduced by the method are shown in Figure 7. All subsequent figures show data reduced by the former method only.

ACCURACY OF THE RESULTS

For the model surface pressure measurements, the maximum percentage reading error, which occurred at the lowest measured pressure, was ± 4.5 per cent. However,

the mean percentage reading error considering all the model surface pressure measurements was ± 1 per cent. The reading errors from all other types of measurements were less than one percent, and the free stream properties obtained from the calibration were known within one per cent.

In calculating the induced pressure increment from the measured pressure, the computation produced about 5-per cent error in the induced pressure increment for a 1-per cent error in measured pressure. Therefore, the approximate mean error in the experimental values for induced pressure increments was ± 5 per cent.

Slide rule accuracy was maintained throughout the computation of the theoretical values. Numerical tables were used from Ref 11, and a chart to determine inviscid cone surface Mach number was employed from Ref 13.

As an additional factor governing the over-all accuracy of the model surface pressure measurements, consideration should be given to the situation where the ends of the pressure leads at the model surface experience a high temperature while the ends at the manometer are at room temperature. The resulting temperature gradient produces a pressure gradient in the line, the magnitude of which strongly depends on the ratio of the mean free path at the model surface to orifice diameter. A discussion by Nagamatsu of this effect can be found in Ref 14. According to Ref 14, temperature conditions similar to those encountered during the experiments reported herein could cause, in some cases, as much as a 6-per cent error in the pressure measurements. This is a most interesting consideration, and an experimental program has been planned by the Air Force's Aeronautical Research Laboratories to determine just how great this effect is for pressure measurements made in the ARL 3-Inch Hypersonic Wind Tunnel. The data included in this report are not modified to take the temperature gradient into account. However, the possibility that such an effect could influence the pressure measurements is mentioned for consideration by the reader.

DISCUSSION

The following discussion will be divided into two sections: (1) results at zero angle of attack, and (2) results at moderate angles of attack.

ZERO ANGLE OF ATTACK

Figure 7 is a plot of induced pressure increment versus distance along the 5-degree cone at Mach 10.72. Two points, one for each of the two different methods of data reduction (see section on data reduction methods), are shown for each experimental pressure measurement. There is a wide difference between the points reduced by the two methods, and the data indicate that those points obtained by using local static pressure seem more reasonable than those obtained according to the method of Baradell and Bertram for the experimental conditions encountered in this paper. In addition to the experimental points, three analytical curves are shown for comparison with the empirical results. The curve obtained from Talbot's method closely agrees with the experimental points, while Probstein's first-order theory for the nonadiabatic case is about 10 per cent above the experimental results. This trend was also noted in Ref 3. The third curve represents Probstein's first-order theory for an insulated cone, and is considerably above the experimental data. This illustrates the strong effect that surface cooling has toward decreasing the induced pressures as compared to an insulated cone.

Figures 8, 9, and 10 show results with the 10-degree cone at three different free stream conditions. For the 10-degree cone, Talbot's method and Probstein's first-order nonadiabatic theory practically coincide with each other, and both agree very well with the experimental results.

Figures 11 through 16 show results with the 15-degree and 20-degree cones for different free stream conditions. An interesting trend indicated here is that Probstein's nonadiabatic theory falls below Talbot's method, and gives closer

agreement to the experimental results. For these cones, all three theoretical curves overestimate the experimental data.

Figures 17 through 20 show the experimental and theoretical values of induced pressure increment correlated by the hypersonic interaction parameter, $\bar{\chi}_c$, and the hypersonic similarity parameter, K . Probstein's first-order theory is, of course, linear in $\bar{\chi}_c$, and the points obtained from Talbot's method so closely approximate a linear relationship with $\bar{\chi}_c$ that a mean straight line can easily be drawn through these points. In general, the experimental data indicate an approximate linear relationship with $\bar{\chi}_c$.

In summary, the experimental results from the cones at zero angle of attack, when compared with theory, indicate that Talbot's method best predicts pressures on the 5-degree cone, both Talbot's method and Probstein's first-order nonadiabatic theory are equally good for the 10-degree cone, and that Probstein's nonadiabatic theory best predicts pressures on the 15-degree and 20-degree cones. As far as actual numerical agreement is concerned, theory predicts the experimental pressures with reasonable accuracy for the 5-degree and 10-degree cones, but is 12 to 28 per cent above the experimental results for the 15-degree and 20-degree cones. As would be expected, the self-induced pressure effect is generally more predominate for the smaller-angle cones than for the larger-angle cones. Also, the results indicate that induced pressures on a cone can be correlated reasonably well by $\bar{\chi}_c$, thus substantiating the experimental trend noted by Talbot et al (Ref 3). Within the range of K and $\bar{\chi}_c$ achieved during the cone investigation, the numerical points computed from Talbot's method indicate that the induced pressure increment is a function only of K and $\bar{\chi}_c$ (See Figures 18 through 21.). Therefore, under these K and $\bar{\chi}_c$ conditions, the amount of computation involved with using Talbot's method may be considerably reduced due to its linear properties.

MODERATE ANGLES OF ATTACK

Figures 21 through 29 are plots of pressure coefficient on the 10-degree, 15-degree, and 20-degree cones versus angle of attack for various free-stream conditions. The maximum angle of attack range is from -15 to 15 degrees. In all cases, the experimental results are compared with Newtonian impact and modified Newtonian theories.

The conclusion from the data is that Newtonian impact theory predicts the experimental pressures on the 10-, 15-, and 20-degree cones quite well within the angle of attack range of $3^{\circ} \leq \alpha \leq 15^{\circ}$. However, at angles of attack less than 3 degrees, Newtonian impact theory does not accurately predict the results. An extrapolation of both the experimental and theoretical curves to higher angles of attack seems to indicate that, in this range, modified Newtonian theory is more accurate than Newtonian impact theory.

Figures 21 through 29 also indicate a variation of pressure coefficient along the surface of the cones, thus illustrating the self-induced pressure effect. If the measured difference between induced pressure and inviscid pressure (both at $\alpha = 0$) is subtracted from the cone pressures at small angles of attack, the results at small α closely approach Newtonian theory. Therefore, the disagreement between experiment and Newtonian theory can be attributed in part to the induced pressure effect.

CONCLUSIONS

The results presented in this report are summarized as follows:

(1) With the cones at zero angle of attack, the experimental results indicate that for the free-stream conditions reported herein, Talbot's method best predicts self-induced pressures on the 5-degree cone, both Talbot's method and Probstein's first-order nonadiabatic theory are equally good for the 10-degree cone and that Probstein's nonadiabatic theory best predicts self-induced pressures on the 15-degree and 20-degree cones.

2. Also at zero angle of attack, the results indicate that the self-induced pressures on cones can be correlated reasonably well by the hypersonic interaction parameter, $\bar{\chi}_c$, for constant values of the hypersonic similarity parameter, K . These results substantiate the experimental trend noted by Talbot (Ref 3).

3. For cones at moderate angle of attack, the results indicate that Newtonian impact theory predicts the pressure coefficient on 10° , 15° , and 20° cones quite well in the range of $3^\circ \leq \alpha \leq 15^\circ$, but was not accurate for angles of attack less than 3 degrees.

REFERENCES

1. Hayes, Wallace D., and Probst, Ronald F.: Hypersonic Flow Theory. Academic Press (New York and London) 1959, pp. 333-374.
2. Probst, Ronald F.: Interacting Hypersonic Laminar Boundary Layer Flow Over a Cone. Div. Eng., Brown University, Tech. Report AF 2798/1, March 1955, Contract AF33(616)-2798.
3. Talbot, Lawrence; Koga, Toyoki; and Sherman, Pauline M.: Hypersonic Viscous Flow Over Slender Cones. NACA TN 4327, University of California, September 1958.
4. Grimminger, G.; Williams, E. P.; and Young, G. B. W.: Lift on Inclined Bodies of Revolution in Hypersonic Flow. Journal of the Aeronautical Sciences, Vol. 17, No. 11, November 1950, pp. 675 - 690.
5. Jack, John R.: Aerodynamic Characteristics of a Slender Cone-Cylinder Body of Revolution at a Mach Number of 3.85. NACA RM E51H17, November 1951, declassified 4 October 1956.
6. Julius, Jerome D.: Measurements of Pressure and Local Heat Transfer on a 20° Cone at Angles of Attack up to 20° for a Mach Number of 4.95. NASA TN D-179, December 1959.
7. Amick, James L.: Pressure Measurements on Sharp and Blunt 5° and 15° Half-Angle Cones at Mach Number 3.86 and Angles of Attack to 100° . NASA TN D-753 (University of Michigan), February 1961.
8. Bogdonoff, S. M., and Vas, I. E.: Experimental Studies at Mach Numbers 12 to 19 of Conical and Blunted Bodies at Zero Angle of Attack. AFOSR TN 58-841 (Princeton University), September 1958.
9. Baldwin, Lawrence C.: Viscous Effects on Static Pressure Distribution for a Slender Cone at a Nominal Mach Number of 5.8. CITGAL Memorandum No. 28, Contract DA-04-495-Ord-19, 14 June 1955.
10. Erickson, Wayne D.: Study of Pressure Distributions on Simple Sharp-Nosed Models at Mach Numbers from 16 to 18 in Helium Flow. NACA TN 4113, October 1957.
11. Massachusetts Institute of Technology, Department of Electrical Engineering, Center of Analysis. Tables of Supersonic Flow Around Cones by the Staff of the Computing Section, under the direction of Zdenek Kopal, Tech. Report No. 11, Cambridge, 1947.
12. Baradell, Donald L., and Bertram, Mitchel H.: The Blunt Plate in Hypersonic Flow. NASA TN D-408, October 1960.
13. Ames Research Staff: Equations, Tables, and Charts for Compressible Flow. NACA 1135, 1953.

REFERENCES (CONT'D)

14. Nagamatsu, Henry T.: Hypersonic Experimental Facilities. High Speed Aerodynamics and Jet Propulsion, Volume VIII, pp. 548 - 551, Princeton University Press, 1961.

APPENDIX A

PROBSTEIN'S THEORY FOR PREDICTING SELF-INDUCED PRESSURES ON CONES

In Ref 2, Probststein has developed an analytical expression for the self-induced pressures in terms of known free-stream conditions and cone angle. Beginning with a concept of the hypersonic flow over a cone as shown in Figure 1, he developed this expression assuming a laminar boundary layer in the weak-interaction field by writing the self-induced pressure as a Taylor series expansion in powers of $\frac{d\delta^*}{dx}$:

$$\frac{P}{P_c} = 1 + \frac{1}{\left(\frac{P_c}{P_\infty}\right)} \left[\frac{d(P/P_\infty)}{d\theta} \right]_{\theta=\theta_c} \left(\frac{d\delta^*}{dx} \right) + \frac{1}{2!} \frac{1}{\left(\frac{P_c}{P_\infty}\right)} \left[\frac{d^2(P/P_\infty)}{d\theta^2} \right]_{\theta=\theta_c} \left(\frac{d\delta^*}{dx} \right)^2 + \dots$$

After a series of steps, the above expression leads to the final result as follows:

$$\frac{P}{P_c} = 1 + F_1(k) d_\infty \bar{\chi}_c + F_2(k) d_\infty^2 \bar{\chi}_c^2 + \dots$$

where,

$F_1(k)$ and $F_2(k)$ are functions only of k

$$k = \theta_c M_\infty$$

$$d_\infty = \frac{0.968}{M_\infty^2} \left(\frac{T_w}{T_\infty} \right) + 0.145(\gamma-1) \quad \begin{array}{l} \text{non} \\ \text{insulated} \end{array}$$

$$\text{or } d_\infty = 0.556(\gamma-1) \text{ insulated}$$

$$\text{and } \bar{\chi}_c = M_c^3 \sqrt{\frac{c}{Re_{cx}}}$$

The above expression for self-induced pressure also assumes a linear viscosity-temperature relationship, and a Prandtl number of 0.725. The inclusion of only the $\bar{\chi}_c$ term constitutes the first-order theory, and the inclusion of both the $\bar{\chi}_c$ and $\bar{\chi}_c^2$ terms constitutes the second-order theory. First-order theory agreed more favorably with the current experimental results than did second-order theory (a trend also noted by Talbot in Ref. 3) and only Probststein's first order theory is included with the figures showing the results of the current study.

APPENDIX B

TALBOT'S NUMERICAL-GRAPHICAL METHOD FOR CALCULATING SELF-INDUCED PRESSURES ON CONE SURFACE

In Ref 3, Talbot et al present a method for predicting self-induced pressures by applying the tangent-cone method to an effective body formed by adding the boundary layer displacement thickness to the geometric cone. At the same time, the interaction effect, i.e., the interdependence of the boundary layer thickness and self-induced pressure, is taken into consideration. Essentially, the method consists of three distinct steps as follows:

(1) Plots are made of M_2 , P_2/P_∞ , T_2/T_∞ and Re_2 as functions of various assumed values of effective cone angle, Θ_2 . The subscript, 2, denotes inviscid quantities at the outer edge of the boundary layer. These inviscid results are obtained from the Kopal Tables (Ref 11).

(2) Since $\Theta_2 = \Theta_c + \Theta_s$, the next step is to calculate the slope of the boundary layer for each value of assumed Θ_2 . The boundary layer equation used by Talbot is:

$$\frac{d\delta^*}{dx} \approx \frac{1}{2} \sqrt{\frac{C}{Re_{2x}}} \left\{ \pi \left(\frac{T_w}{T_2} - \frac{\sigma(\gamma-1)}{4} M_2^2 \right) - \left[1 + \sigma^{\frac{1}{3}} \left(\frac{T_w}{T_2} - \frac{T_{aw}}{T_2} \right) \right] \right\}$$

where

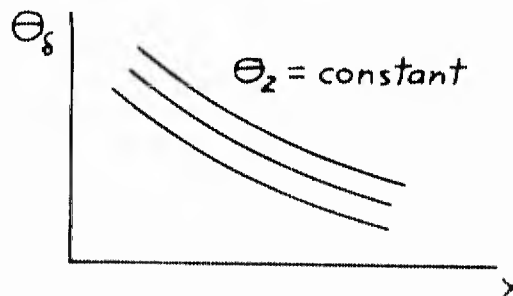
$$\frac{T_{aw}}{T_2} = 1 + \sigma^{\frac{1}{2}} \frac{(\gamma-1)}{2} M_2^2$$

and σ = Prandtl number.

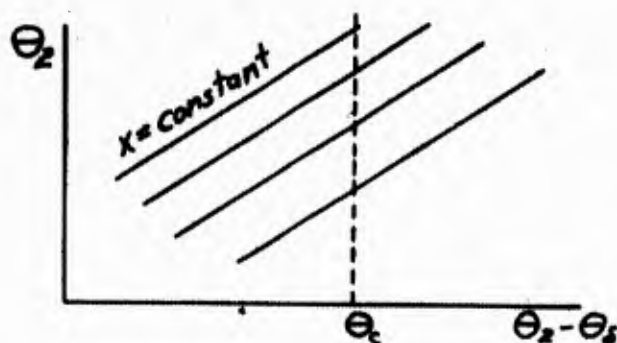
Using the small angle approximation, we have

$$\Theta_s = \tan^{-1} \frac{d\delta^*}{dx} \approx \frac{d\delta^*}{dx}$$

The results are plotted as shown below.



(3) The final step is simply a cross-plot of information obtained in step (2). The cross-plot is shown below:



From the above plot, the effective body slope, Θ_2 , can be found as a function of x for a given cone model of angle Θ_c . The tangent-cone method is then applied to the effective body, and with the use of Ref 11, the induced pressures are determined for the cone of angle Θ_c .

APPENDIX C

BARADELL-BERTRAM METHOD OF ADJUSTING PRESSURES MEASURED IN A CONICAL FLOW FIELD

In Ref 12, Baradell and Bertram have discussed the general problem of adjusting pressure data originally obtained in a conical flow field to correlate with similar data obtained in a uniform flow field. They have presented a relation which involves the subtraction of the pressure increment induced by the nozzle pressure gradient from the conical flow pressure distribution. In particular, the relation is

$$\left(\frac{P}{P_{\infty}}\right)_{\text{uniform flow}} = \left(\frac{P}{P_n}\right)_{\text{conical flow}} - \left(\frac{P_e - P_n}{P_n}\right)_{\text{conical flow}}$$

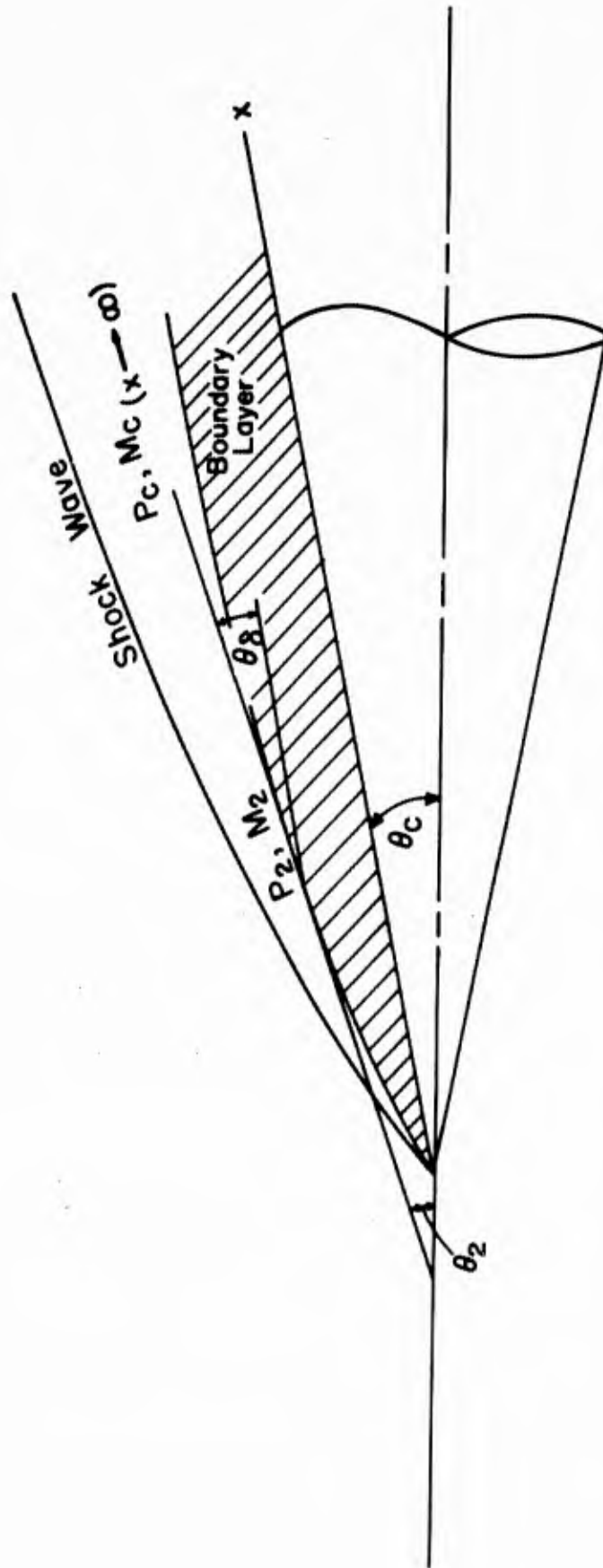
where

p = measured pressure

p_{∞} = static pressure in a uniform-flow nozzle

P_n = static pressure just ahead of the model nose in a conical-flow nozzle

P_e = local free-stream static pressure in conical-flow nozzle



Not to Scale

Figure 1. Diagram of the flow model used for analyzing hypersonic flow over cones.

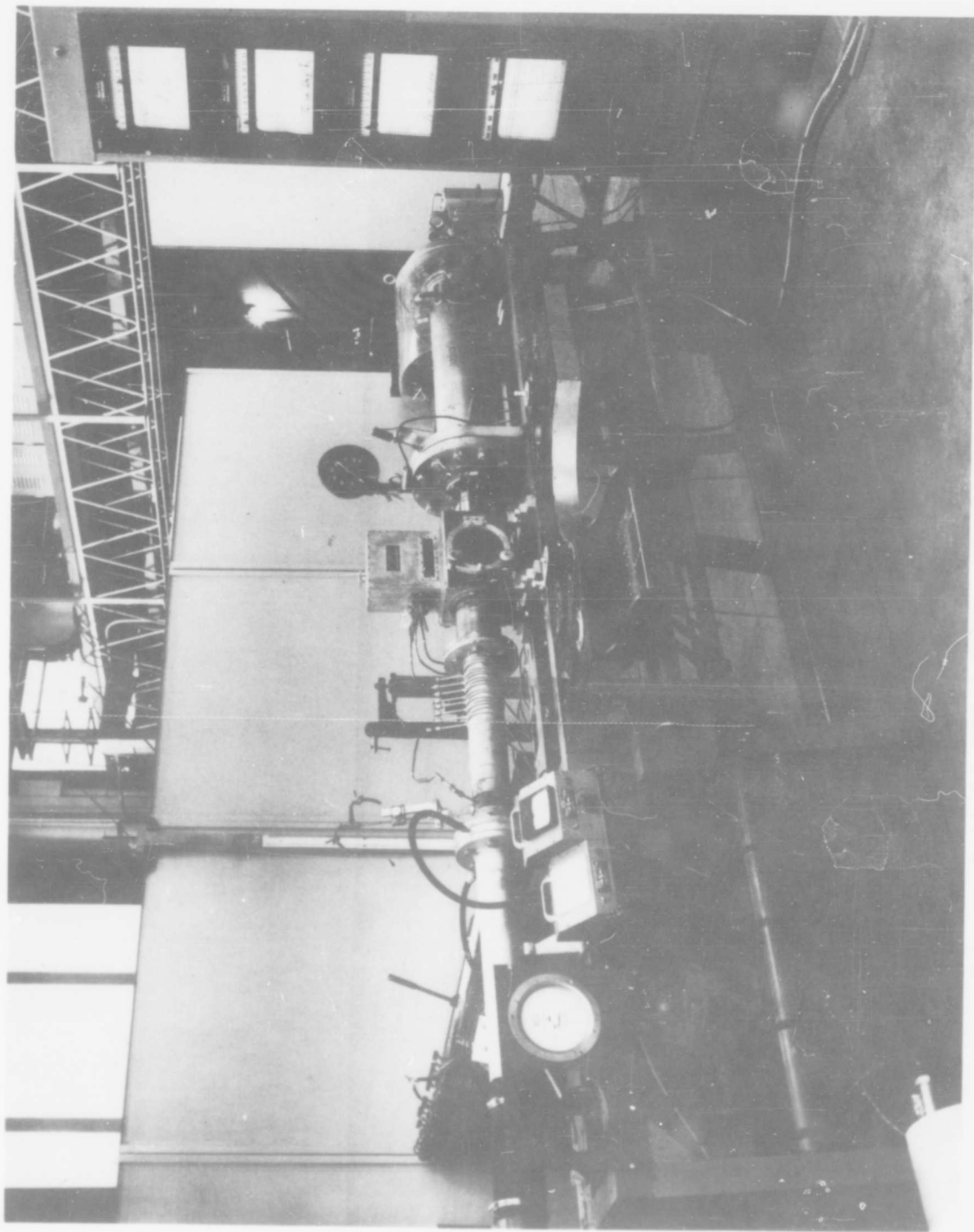


Figure 2. ARL 3-inch Hypersonic Wind Tunnel. Flow is from right to left.

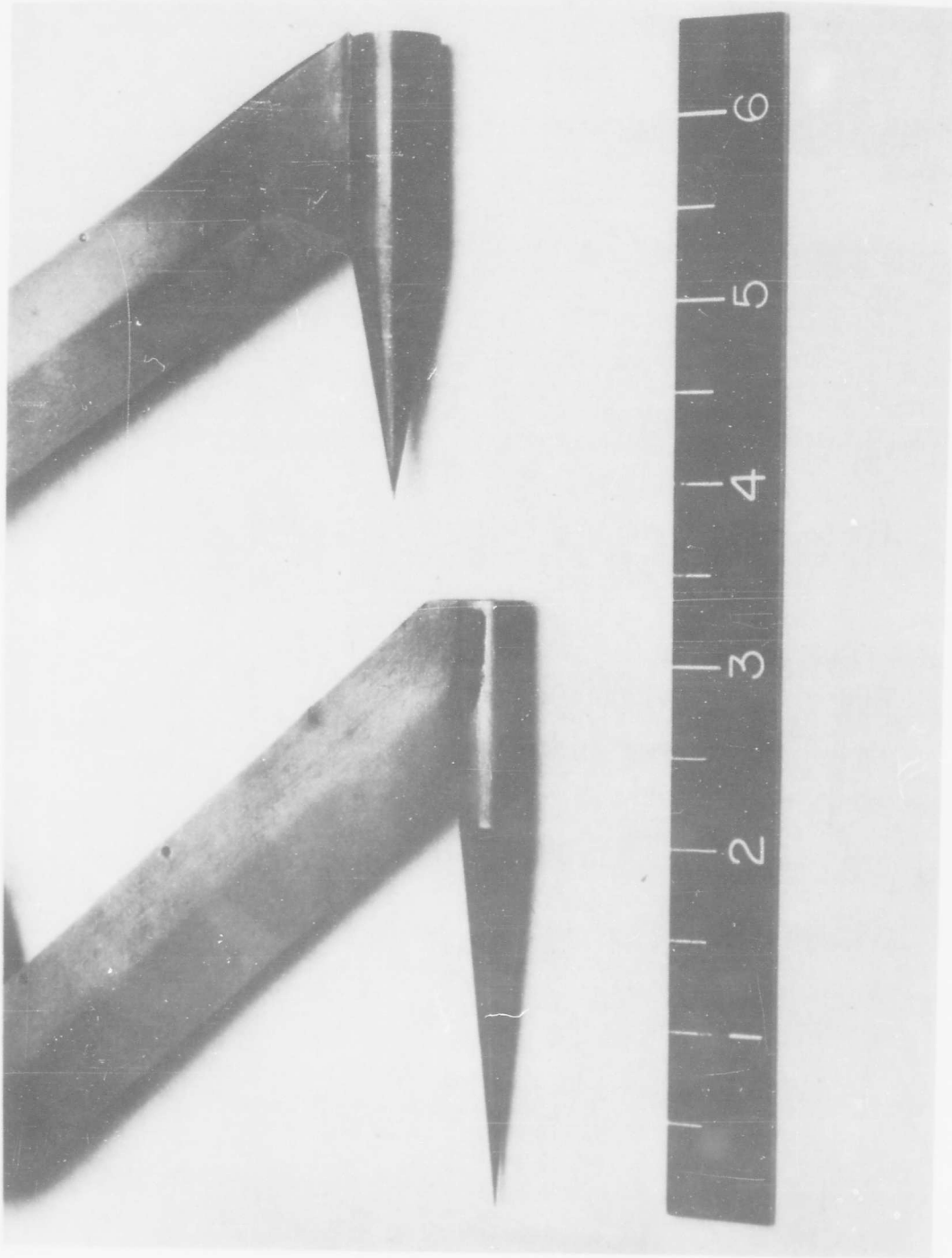


Figure 3. 5-degree (left) and 10-degree (right) semi-vertex angle cone models. Dark surface coloring is due to high temperature oxidation during test runs.



Figure 4. 15-degree (left) and 20-degree (right) semivertex angle cone models

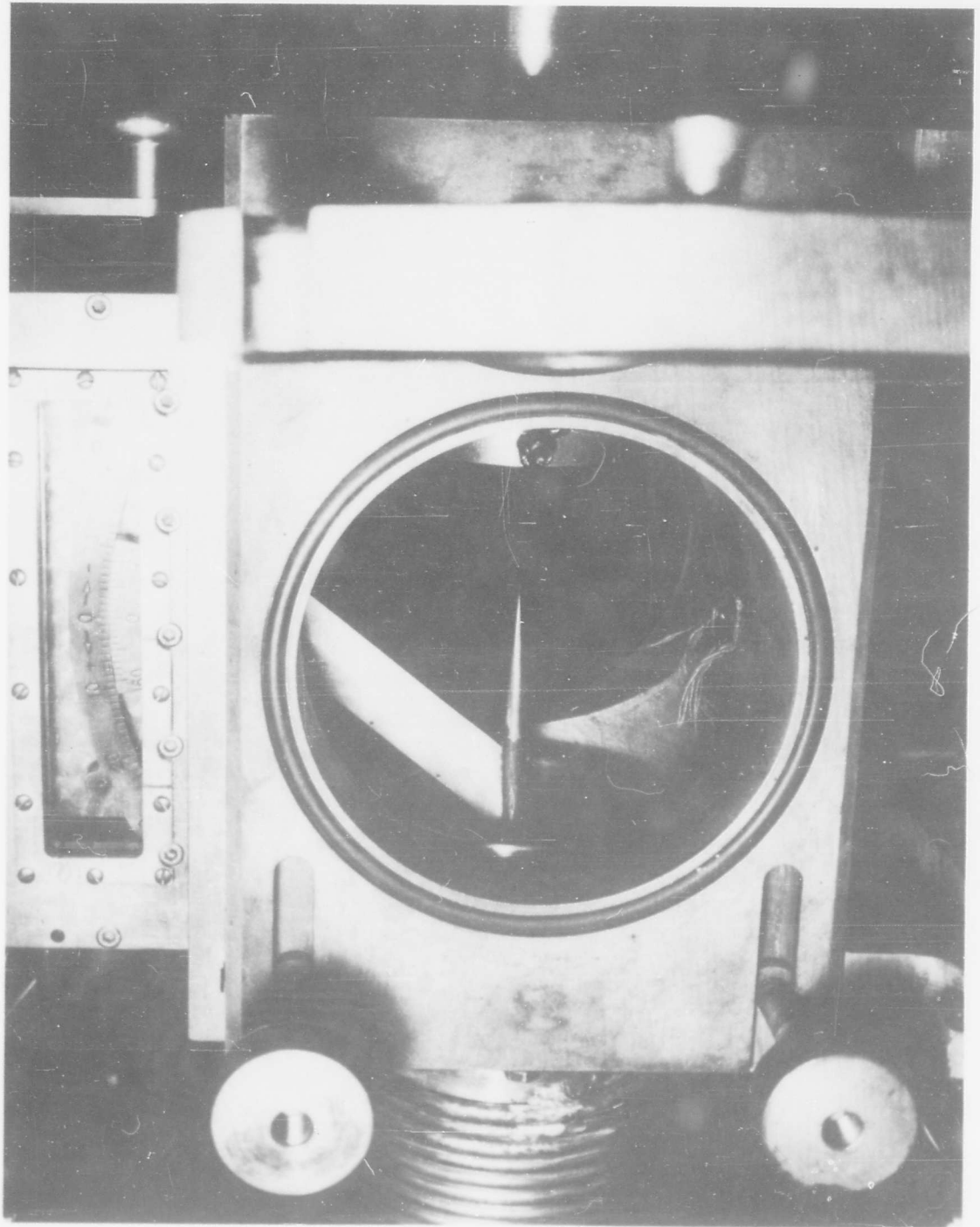


Figure 5. 5-degree model in test section of ARL 3-inch Hypersonic Wind Tunnel. Note model pitching mechanism above test cabin.

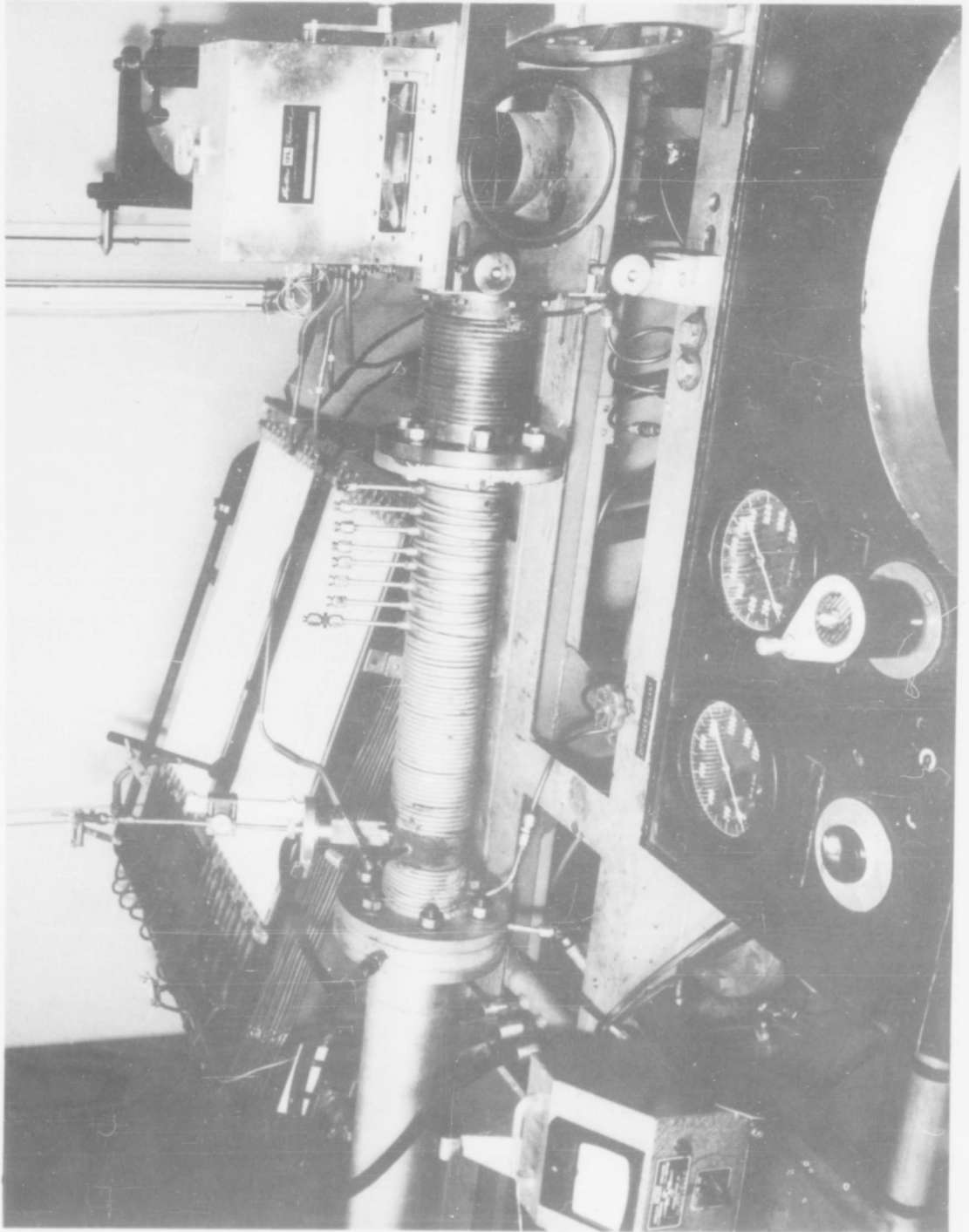


Figure 6. A view of the 3-inch Hypersonic Wind Tunnel showing the inclined silicone oil manometer in the background.

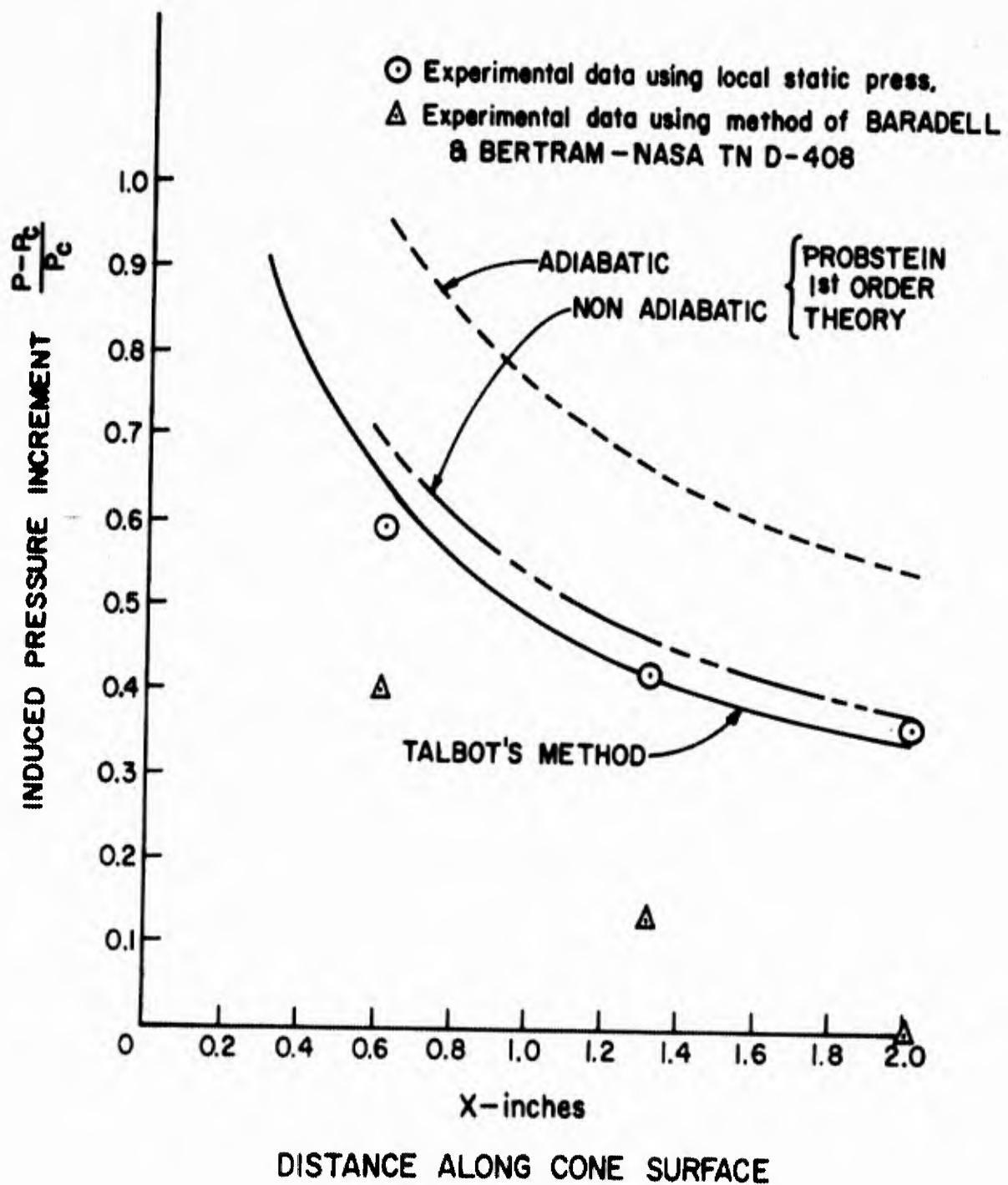


Figure 7. Viscous interaction effects on the 5° cone; $M = 10.72$,
 $Re = 1.88 \times 10^5$ per ft; $T_w/T_\infty = 11.8$

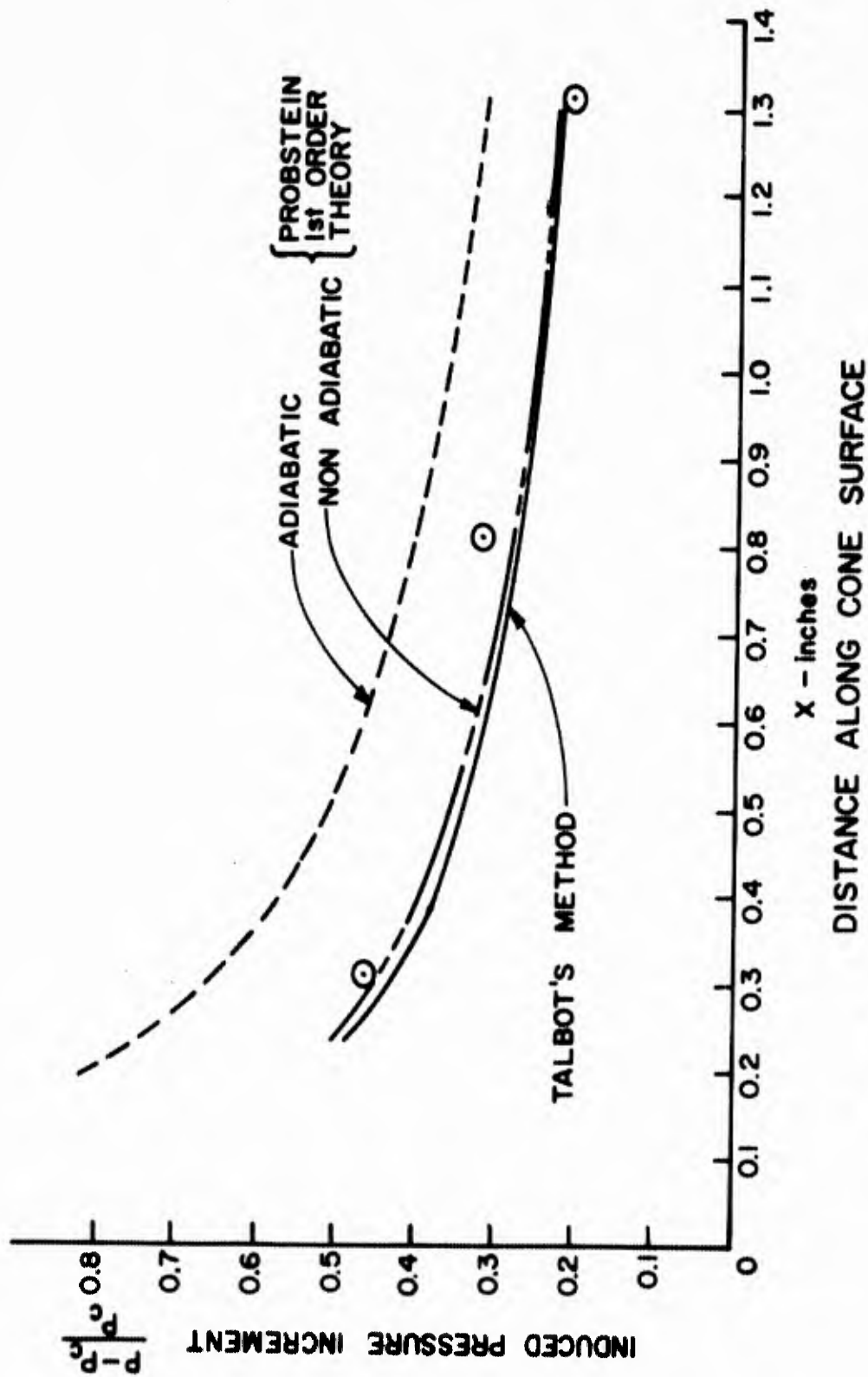


Figure 8. Viscous interaction effects on the 10° cone; $M = 10.72$;
 $Re = 1.88 \times 10^5$ per ft; $T_w/T_\infty = 13.4$

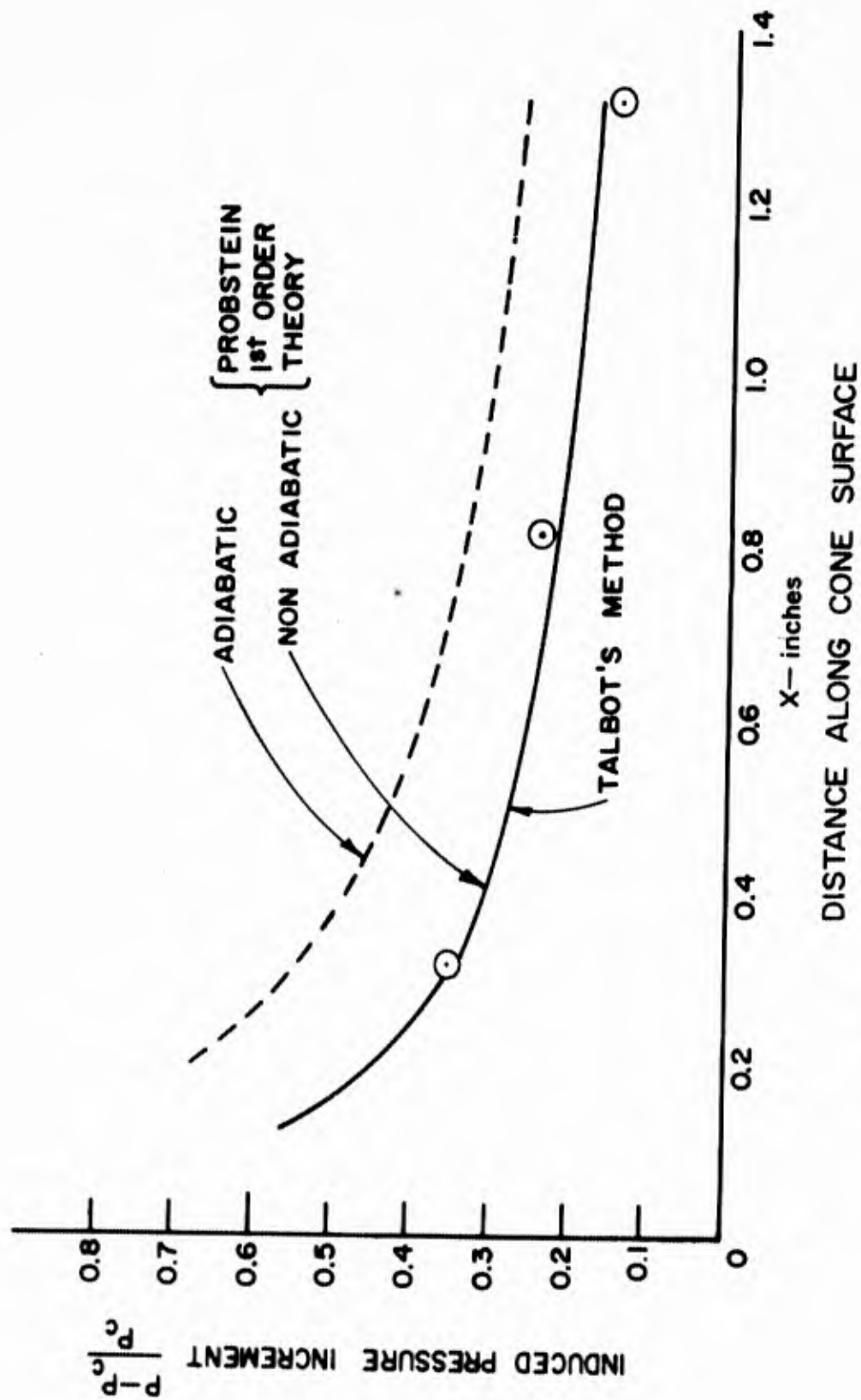


Figure 9. Viscous interaction effects on the 10° cone; $M = 10.86$
 $Re = 2.86 \times 10^5$ per ft; $T_w/T_\infty = 13.9$

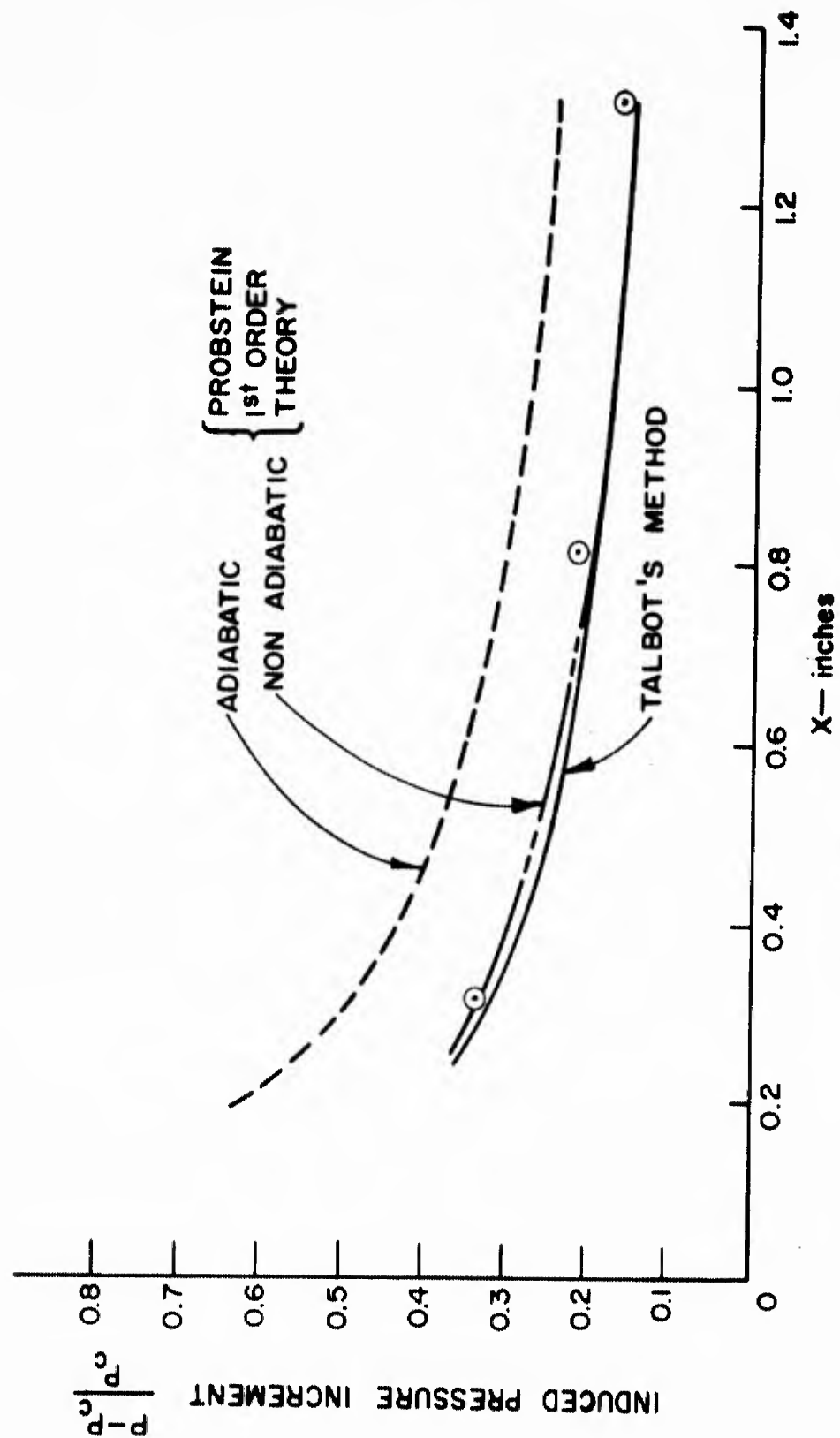


Figure 10. Viscous interaction effects on the 10° cone; $M = 10.95$; $Re = 3.58 \times 10^5$ per ft; $T_w/T_\infty = 14.3$

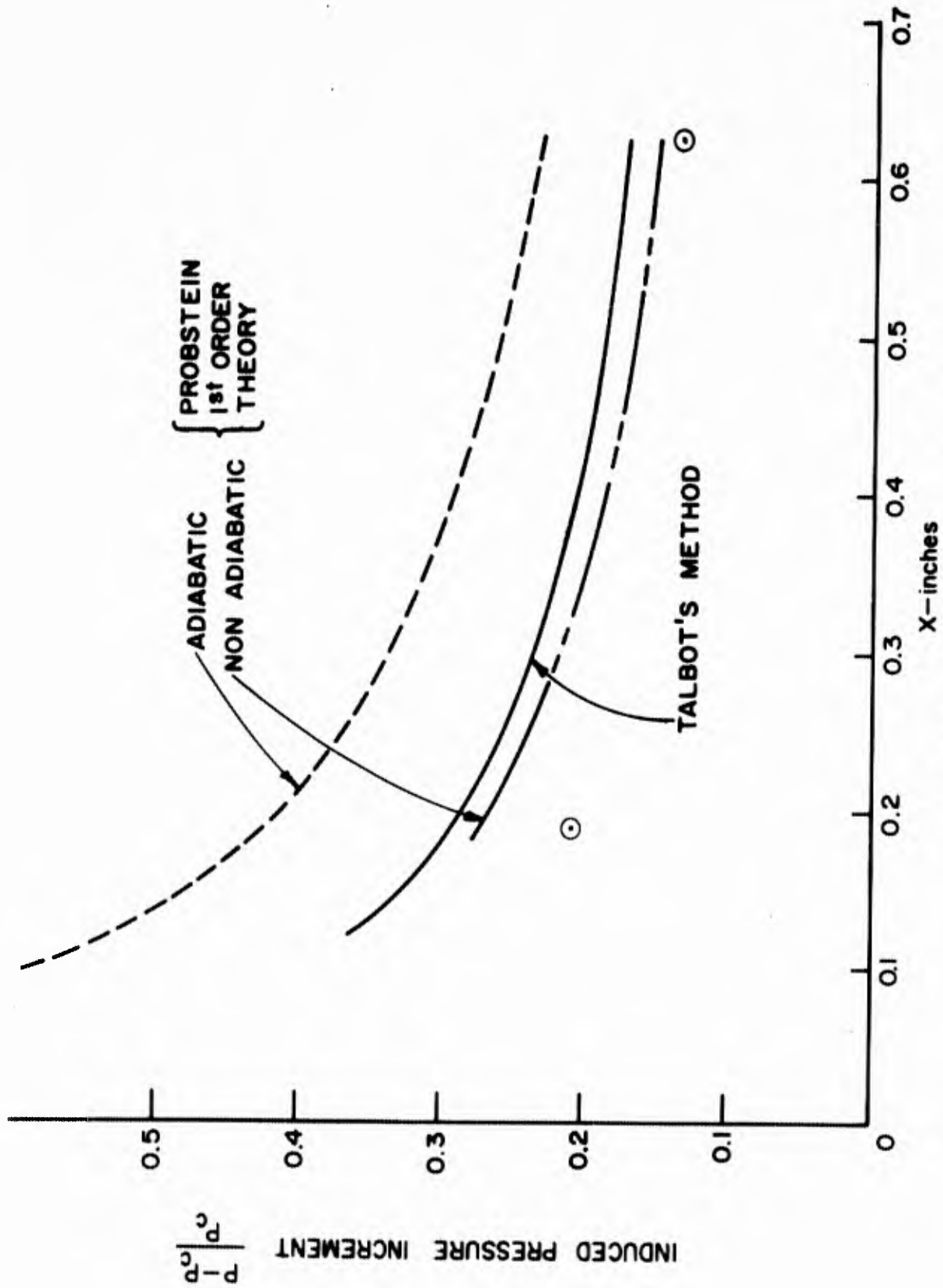


Figure 11. Viscous interaction effects on the 15° cone; $M = 10.72$;
 $Re = 1.88 \times 10^5$ per ft; $T_w/T_\infty = 12.0$

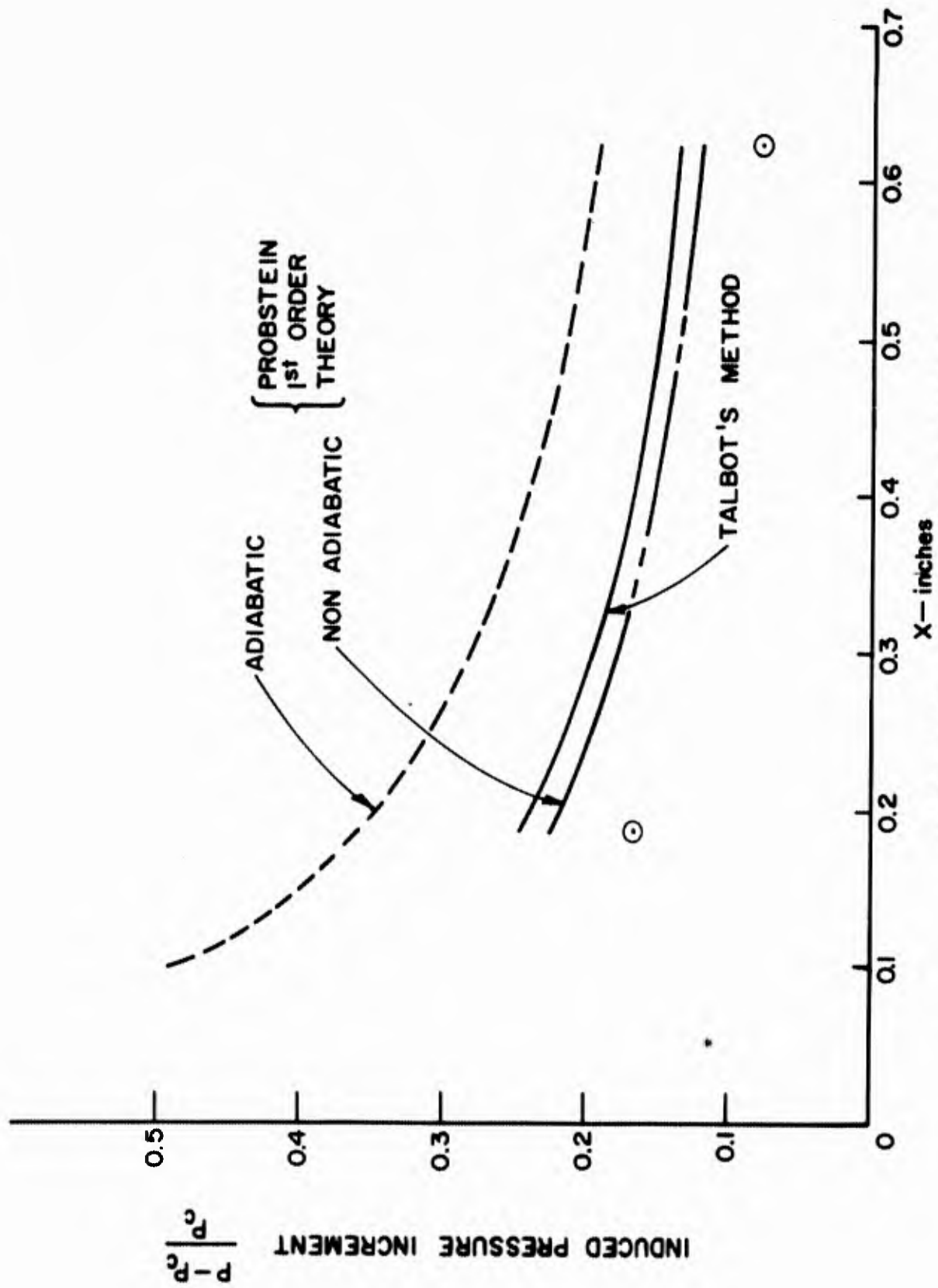
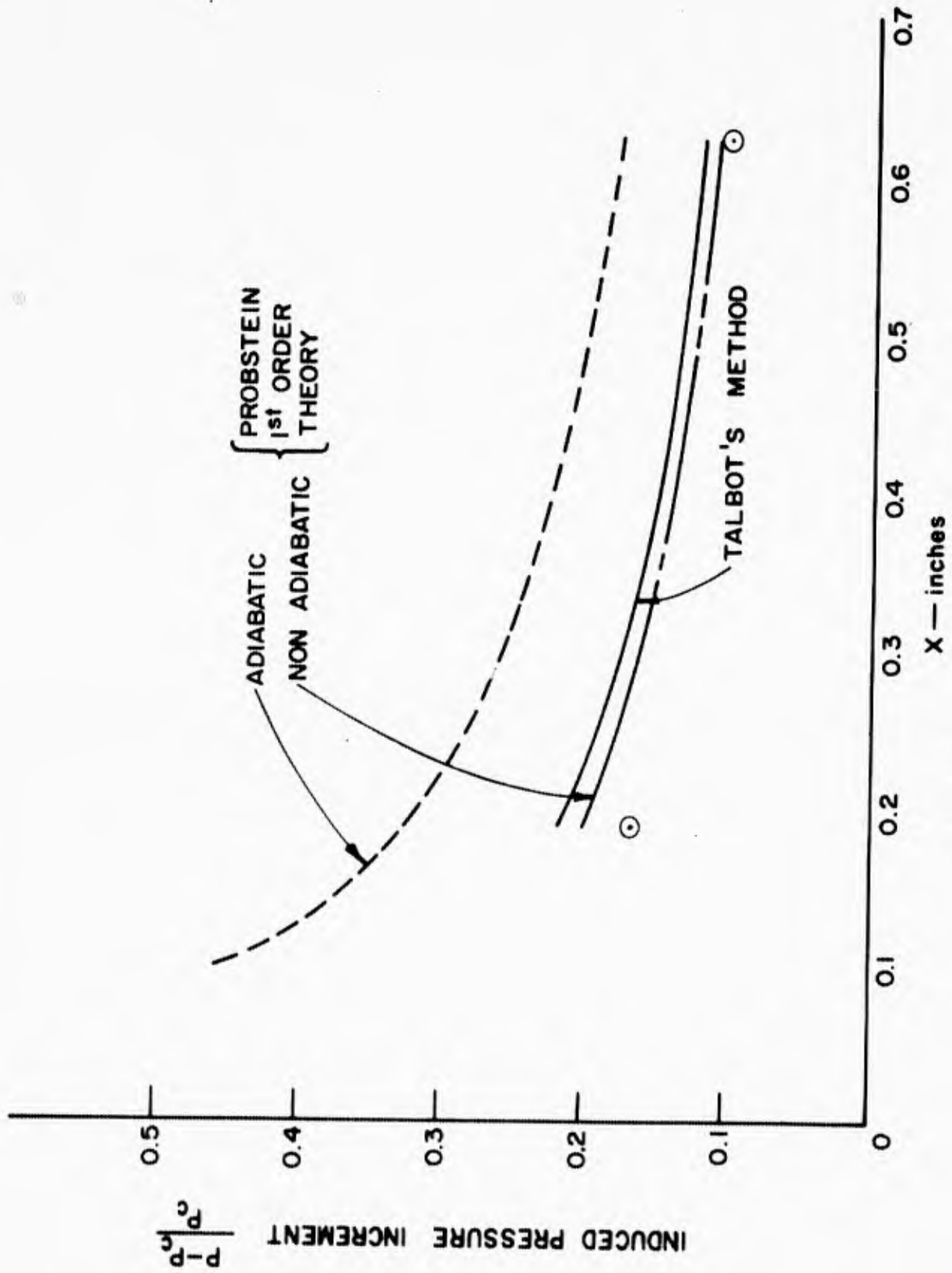


Figure 12. Viscous interaction effects on the 15° cone; $M = 10.86$;
 $Re = 2.86 \times 10^5$ per ft; $T_w/T_\infty = 12.6$



DISTANCE ALONG CONE SURFACE

Figure 13. Viscous interaction effects on the 15° cone; $M = 10.95$; $Re = 3.58 \times 10^5$ per ft; $T_w/T_\infty = 12.8$

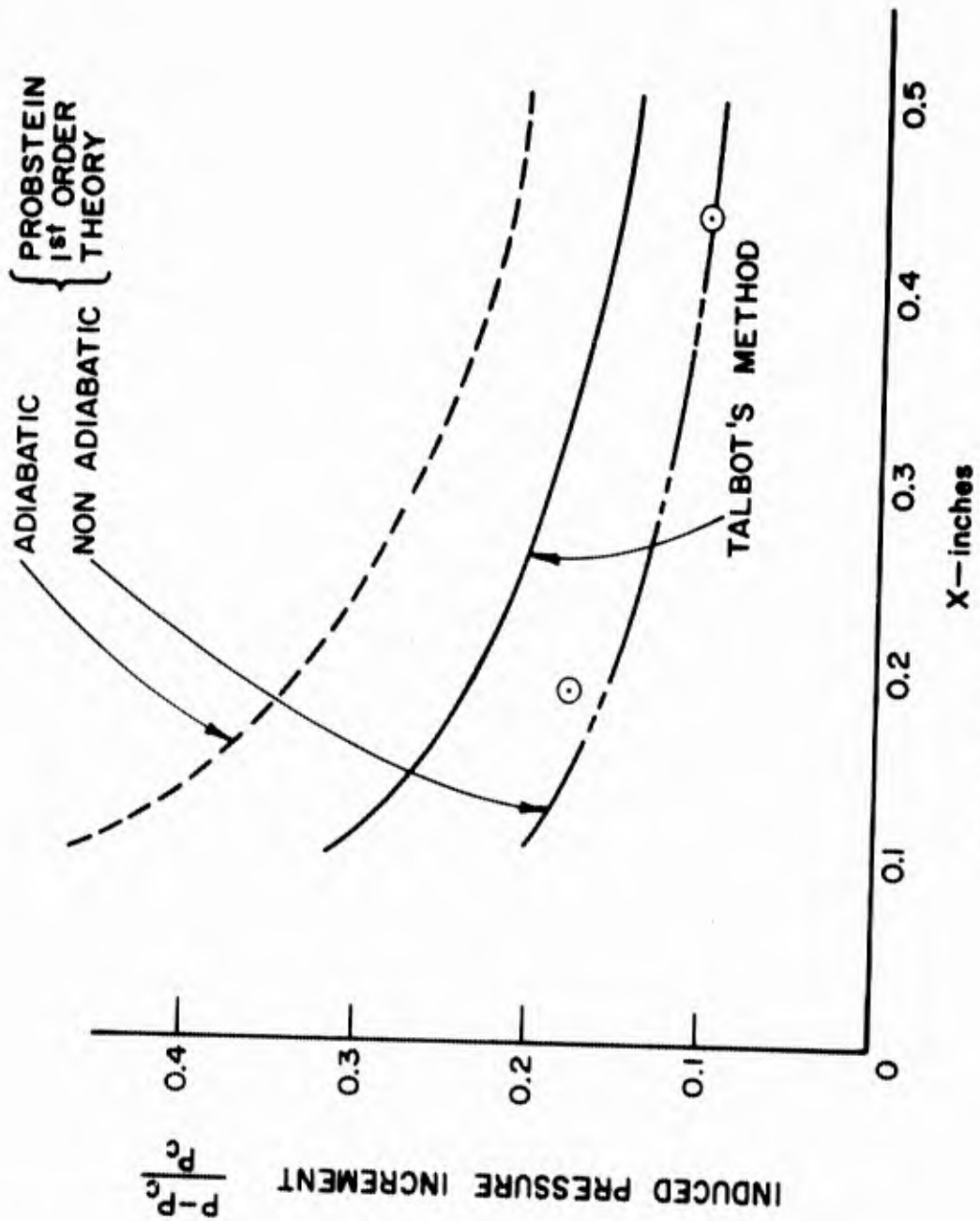


Figure 14. Viscous interaction effects on the 20° cone; $M = 10.72$; $Re = 1.88 \times 10^5$ per ft; $T_w/T_\infty = 14.0$

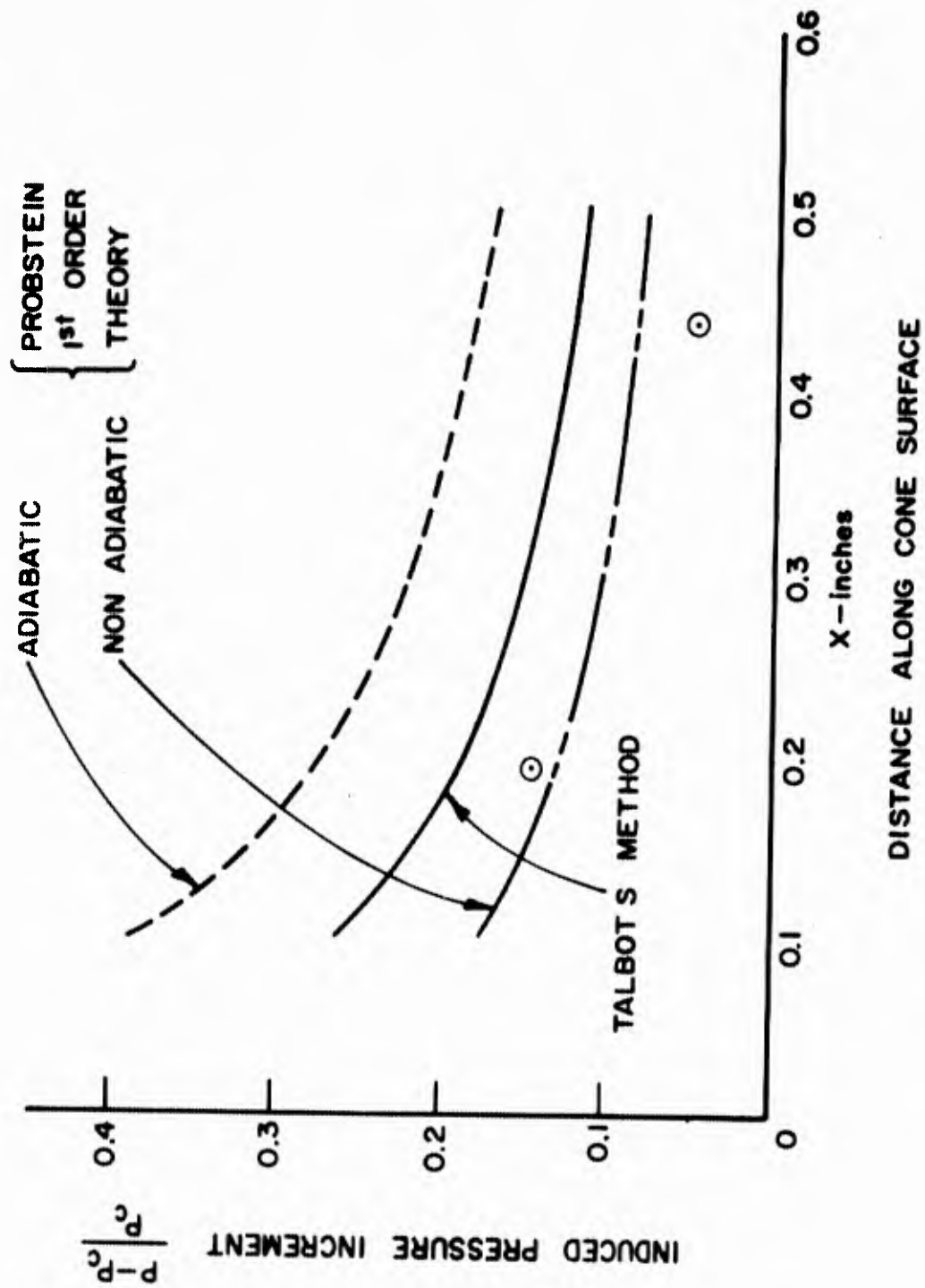


Figure 15. Viscous interaction effects on the 20° cone; $M = 10.82$;
 $Re = 2.86 \times 10^5$ per ft; $T_w/T_{\infty} = 15.0$

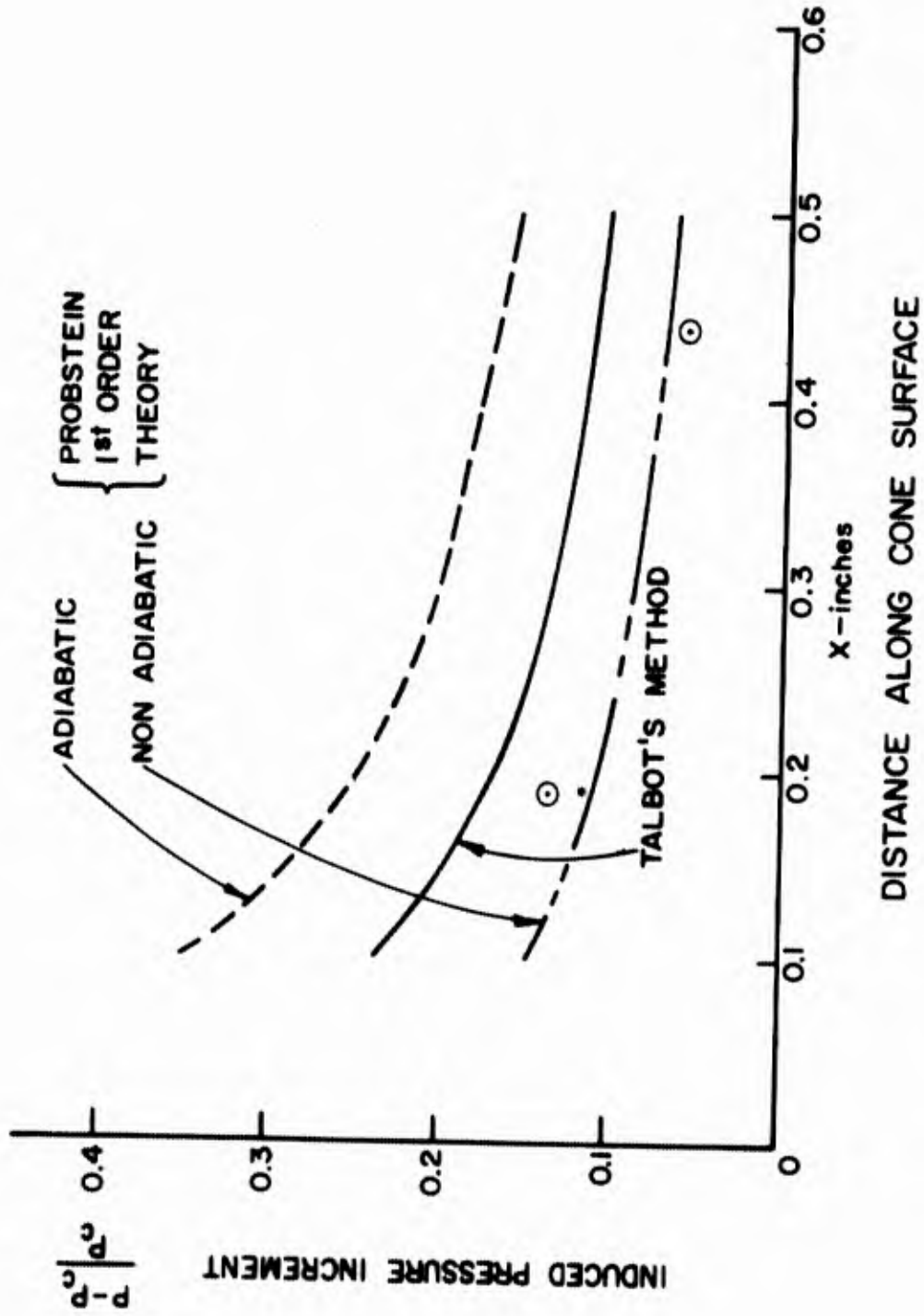


Figure 16. Viscous interaction effects on the 20° cone; $M = 10.95$;
 $Re = 3.58 \times 10^5$ per ft; $T_w/T_\infty = 15.0$

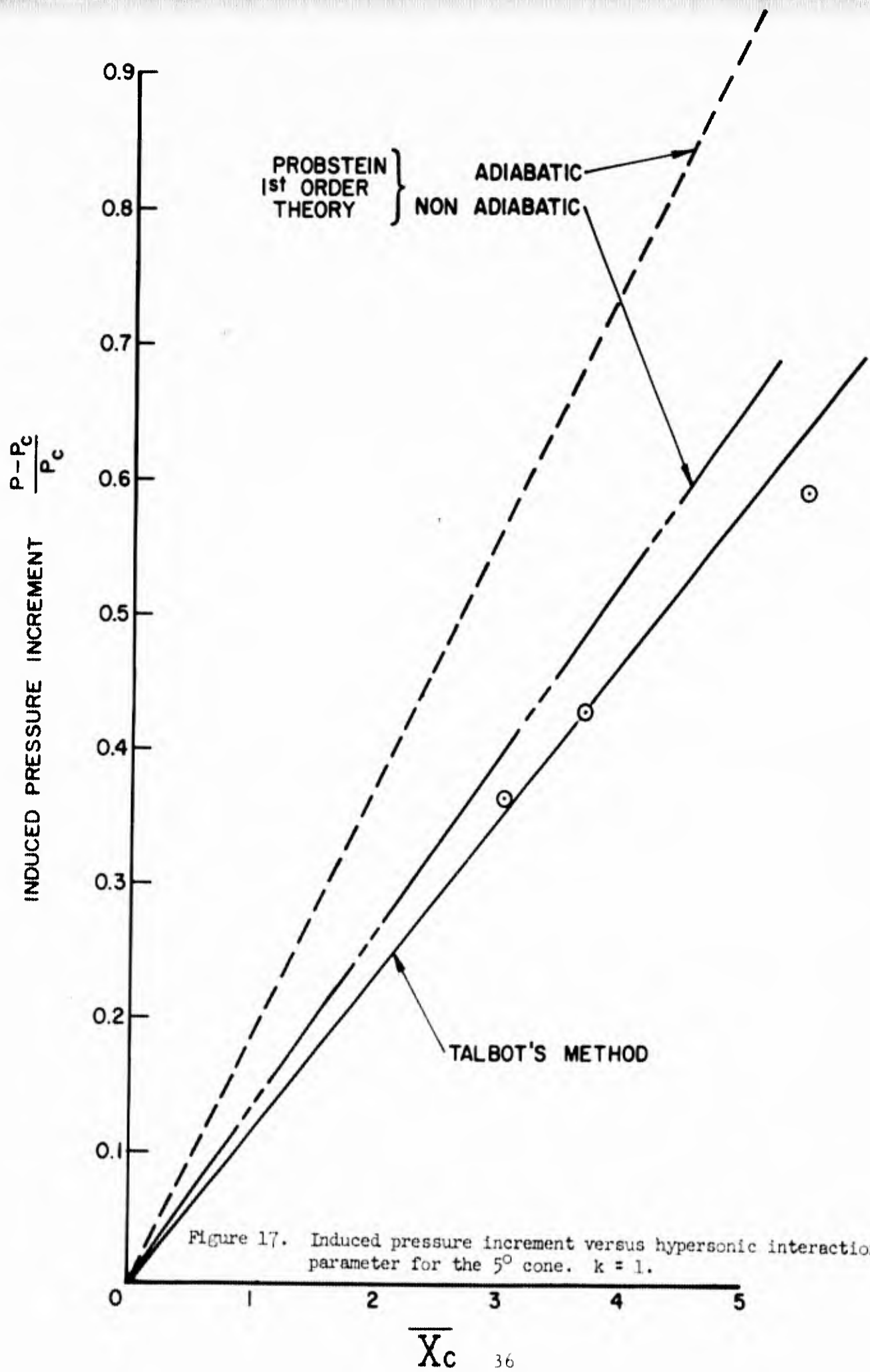


Figure 17. Induced pressure increment versus hypersonic interaction parameter for the 5° cone. $k = 1$.

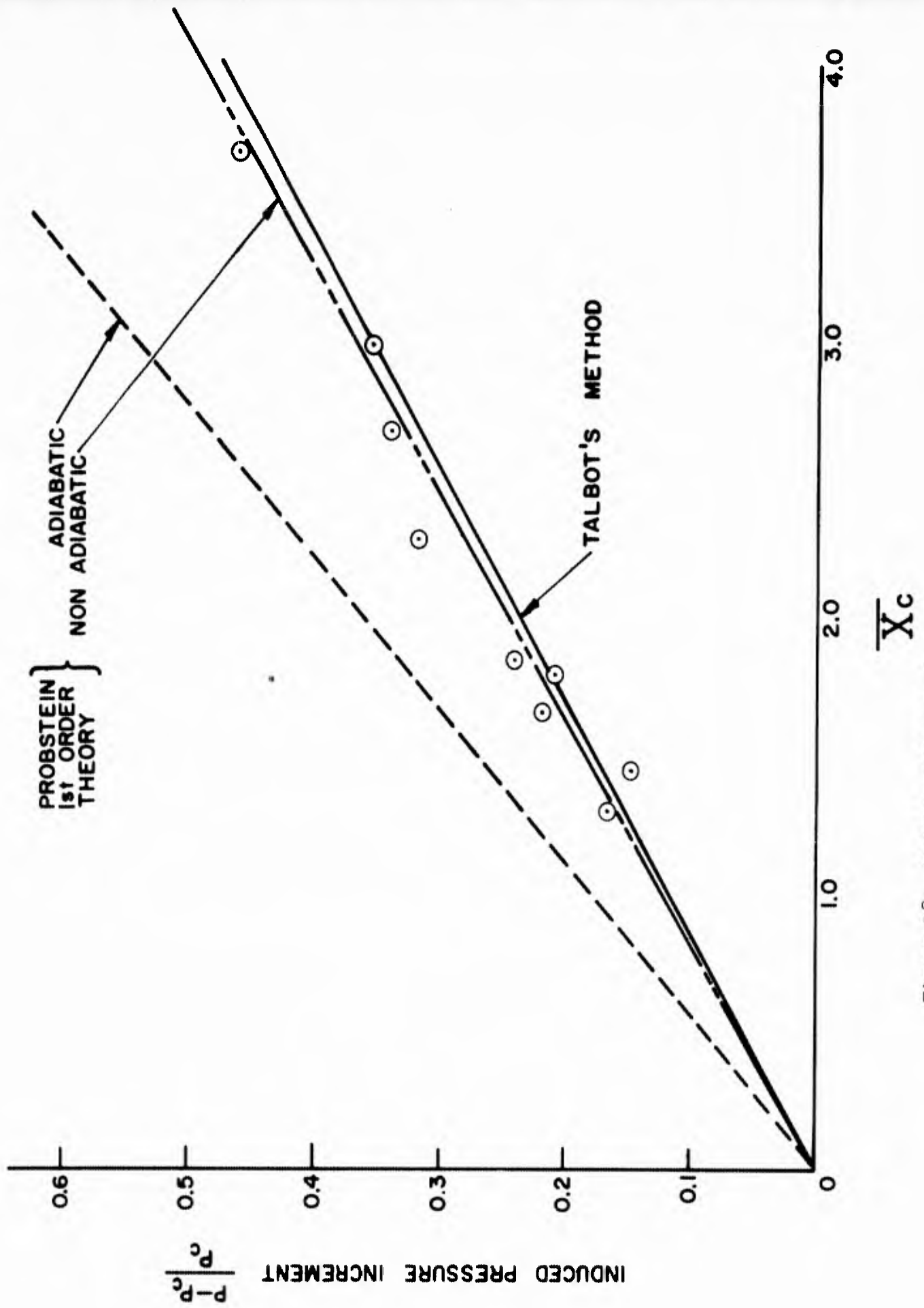


Figure 18. Induced pressure increment versus hypersonic interaction parameter for the 10° cone. $k = 1.9$

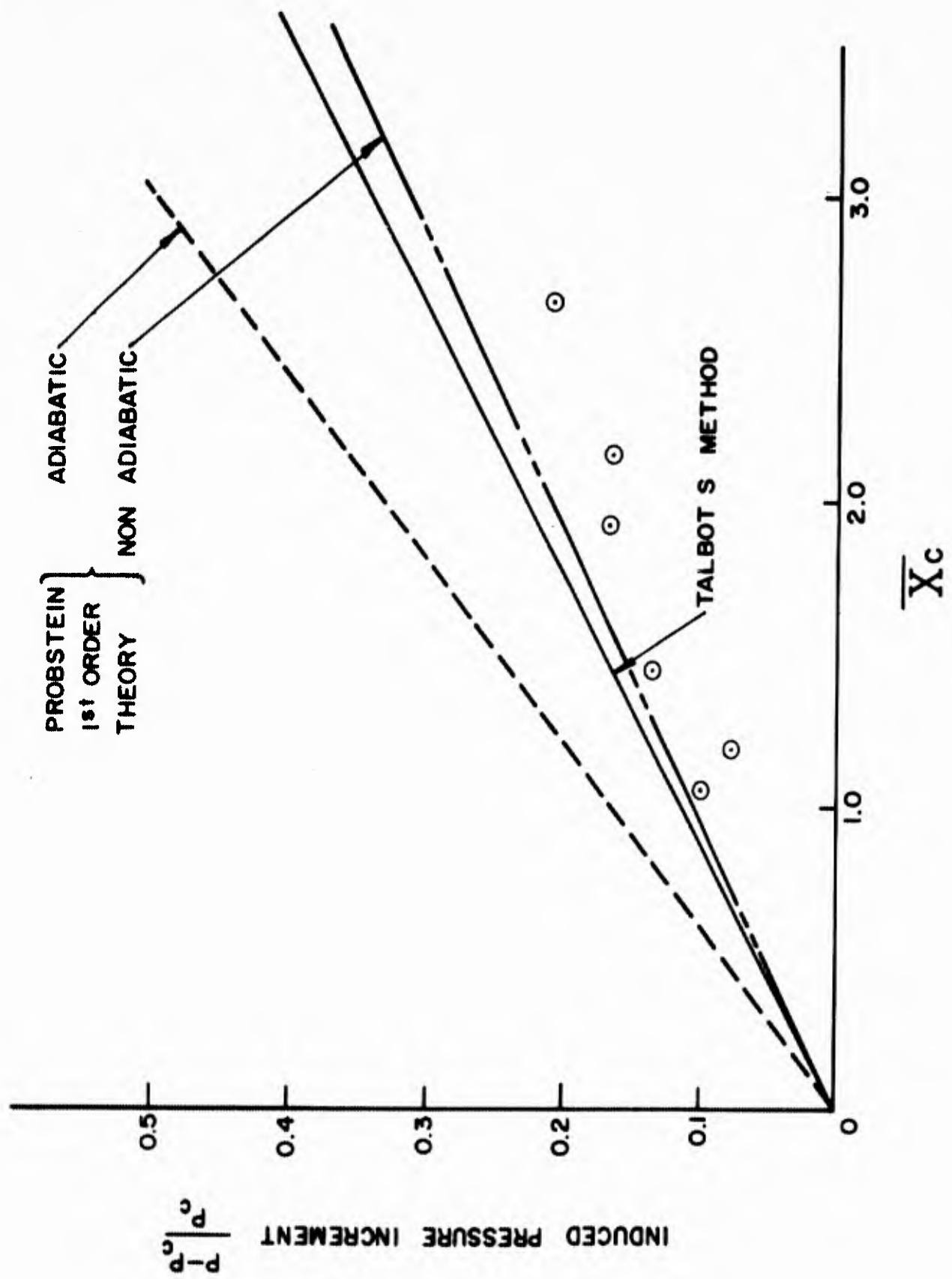


Figure 19. Induced pressure increment versus hypersonic interaction parameter for the 15° cone. $k = 2.9$.

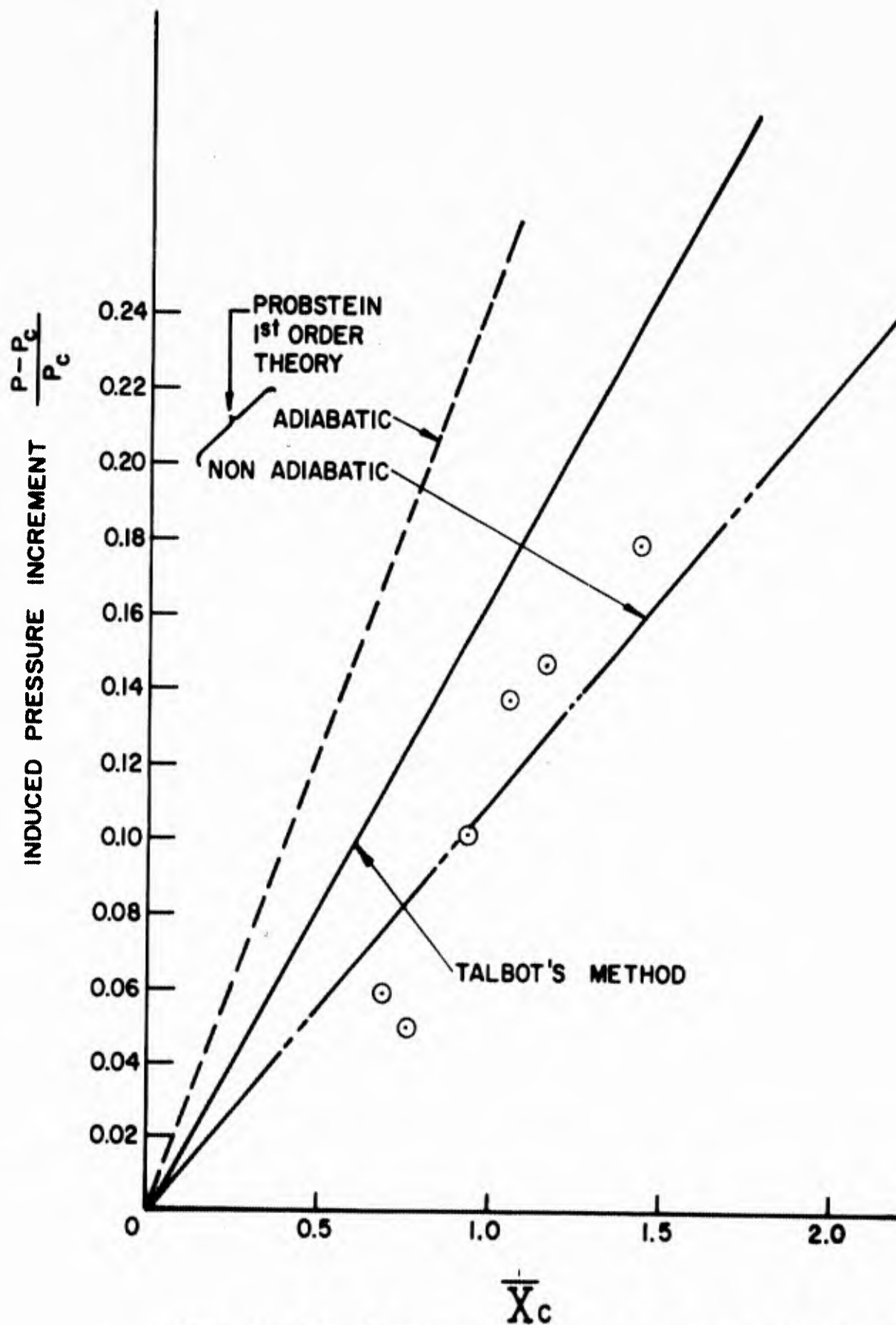
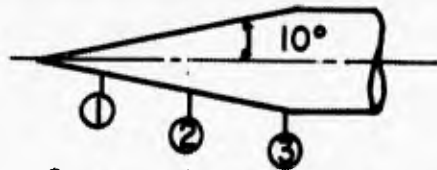


Figure 20. Induced pressure increment versus hypersonic interaction parameter for the 20° cone. $k = 3.8$.



Cone model and orifice location

Code:

- ORIFICE 1 5/16" from vertex
- △ ORIFICE 2 13/16" from vertex
- ORIFICE 3 15/16" from vertex

$$C_p = \frac{2}{\gamma M^2 \omega} \left(\frac{P}{P_\infty} - 1 \right)$$

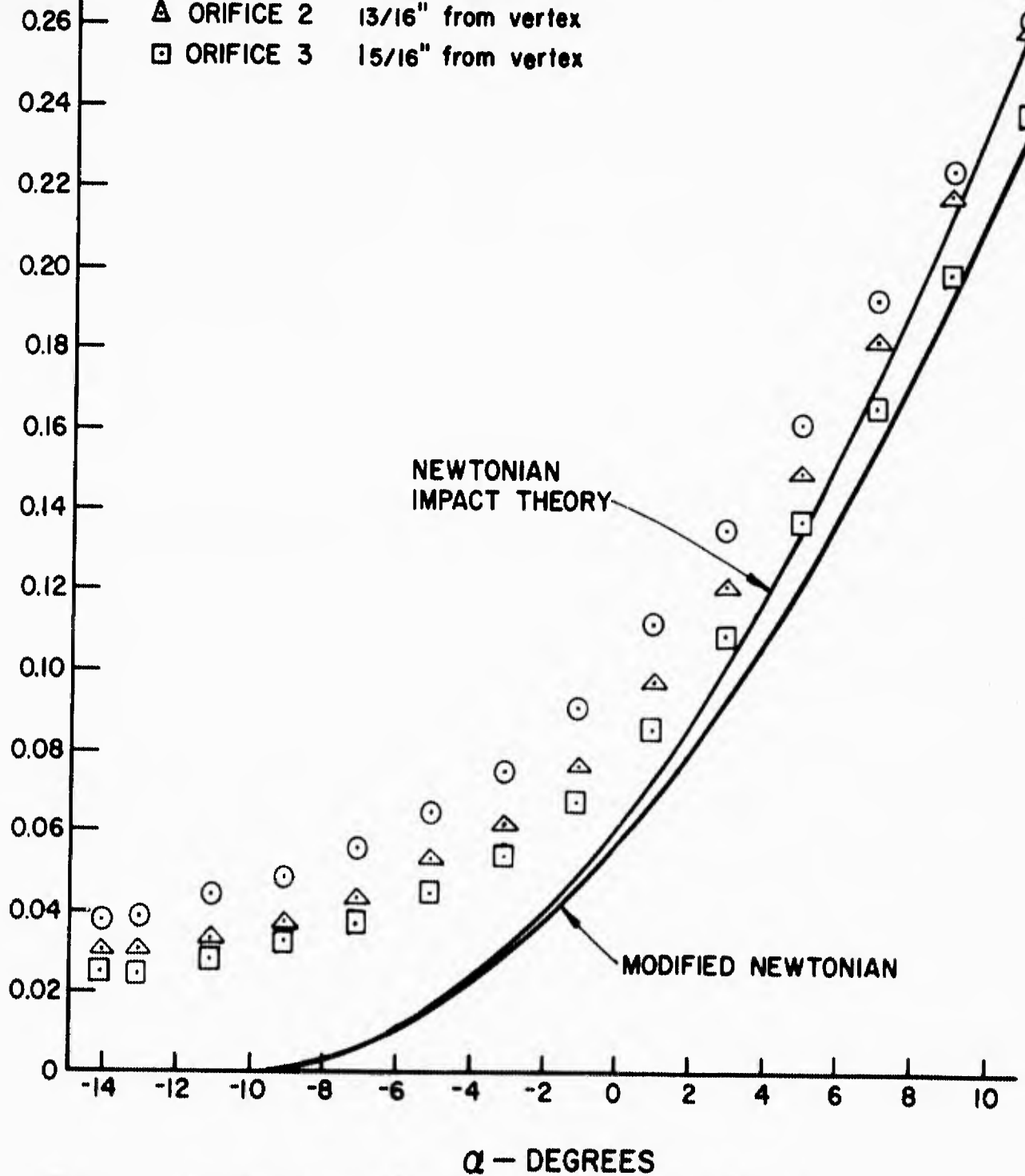
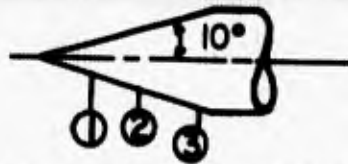


Figure 21. Pressure coefficient versus angle of attack for the 10° cone; $M = 10.72$; $Re = 1.88 \times 10^5$ per ft.



Cone model and orifice location

Code:
 ○ ORIFICE 1 5/16" from vertex
 △ ORIFICE 2 13/16" from vertex
 □ ORIFICE 3 15/16" from vertex

$$C_p = \frac{2}{\gamma M^2 \omega} \left(\frac{P}{P_\infty} - 1 \right)$$

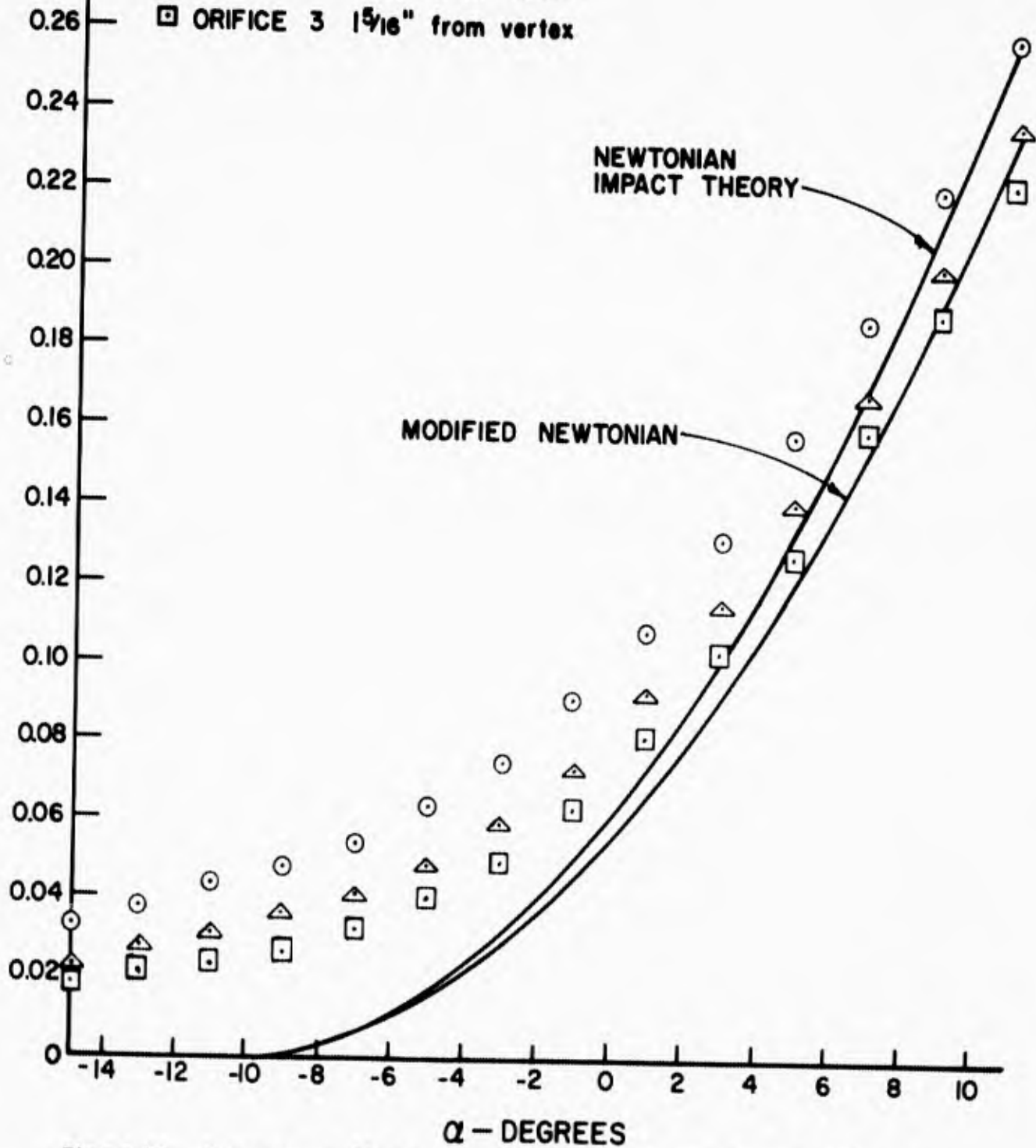
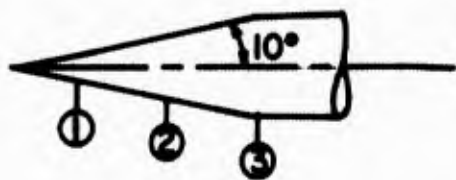


Figure 22. Pressure coefficient versus angle of attack for the 10° cone; $M = 10.86$; $Re = 2.86 \times 10^5$ per ft.



Cone model and orifice location

Code:

- ORIFICE 1 5/16" from vertex
- △ ORIFICE 2 13/16" from vertex
- ORIFICE 3 15/16" from vertex

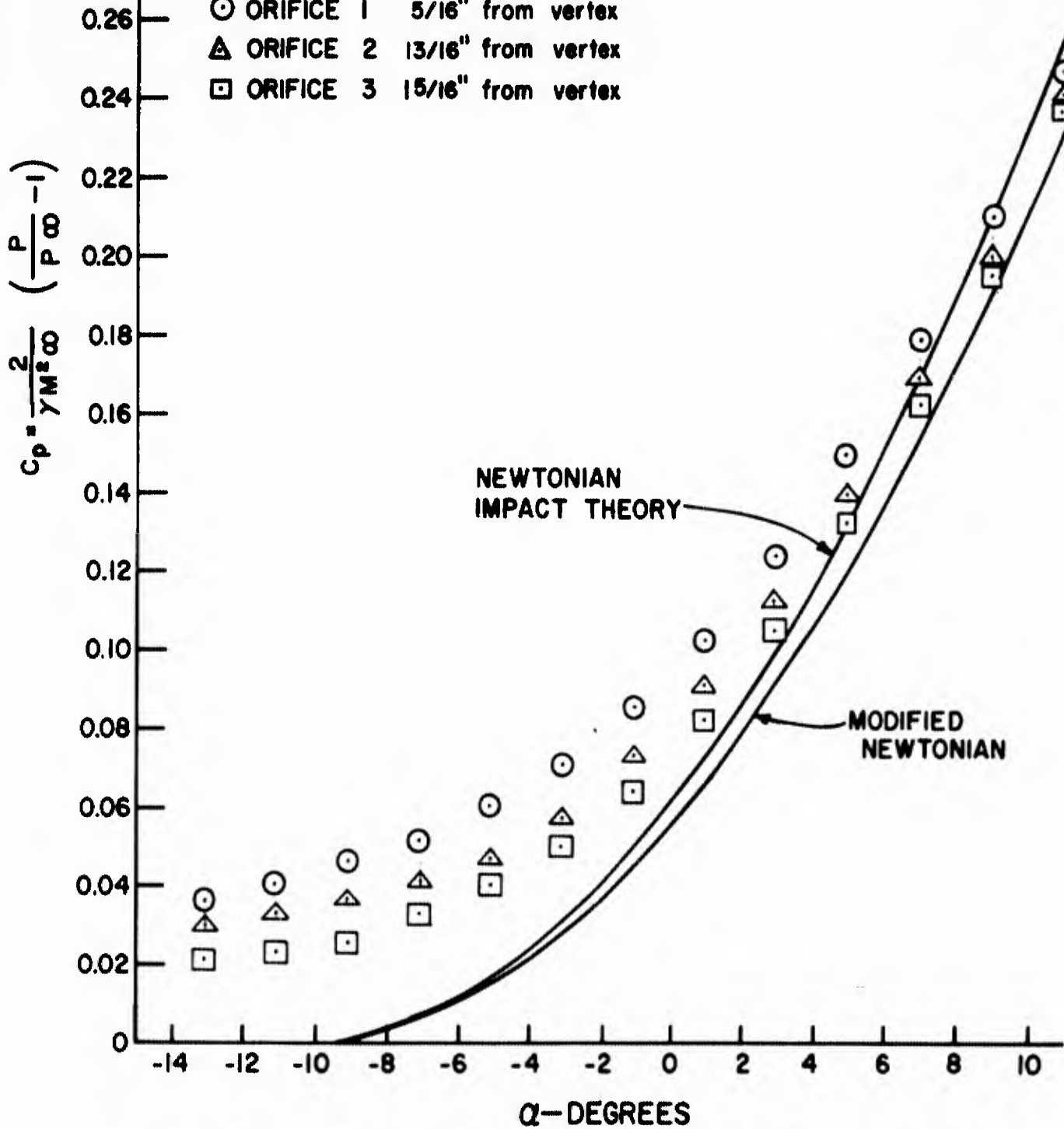


Figure 23. Pressure coefficient versus angle of attack for the 10° cone; $M = 10.95$; $Re = 3.58 \times 10^5$ per ft.

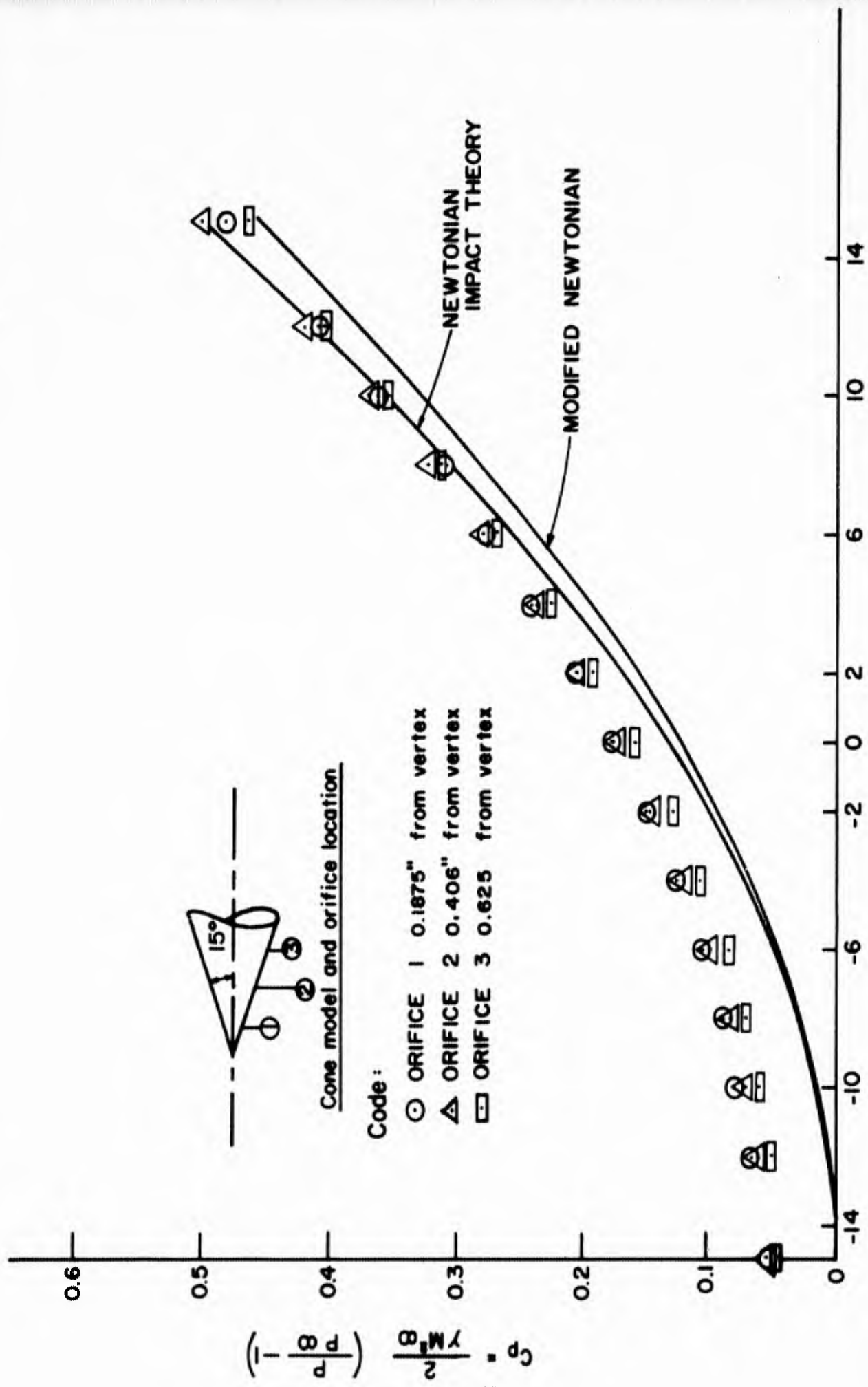


Figure 24. Pressure coefficient versus angle of attack for the 15° cone;
 M = 10.72; Re = 1.88 x 10⁵ per ft.

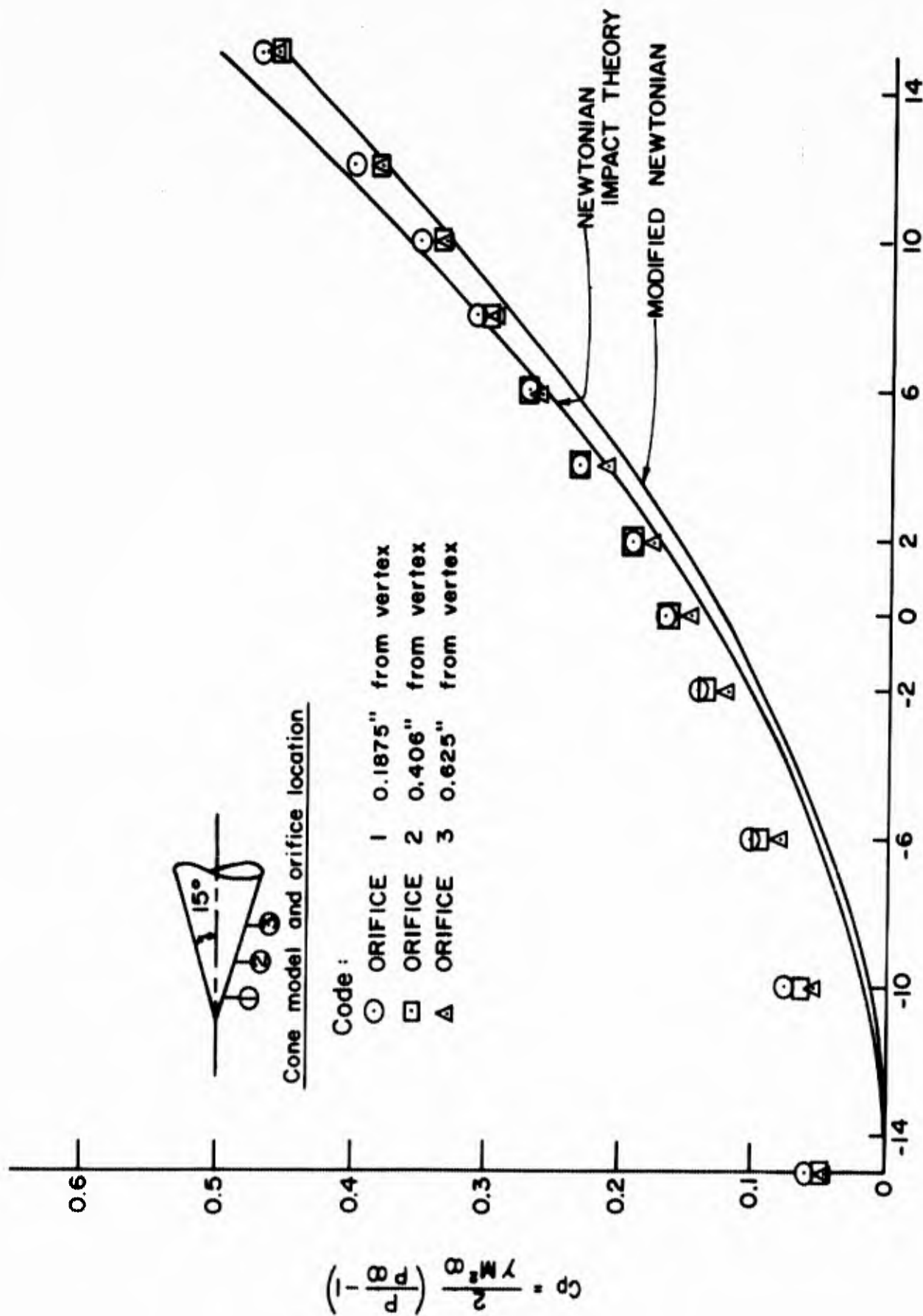


Figure 25. Pressure coefficient versus angle of attack for the 15° cone; M = 10.86; Re = 2.86 x 10⁵ per ft.

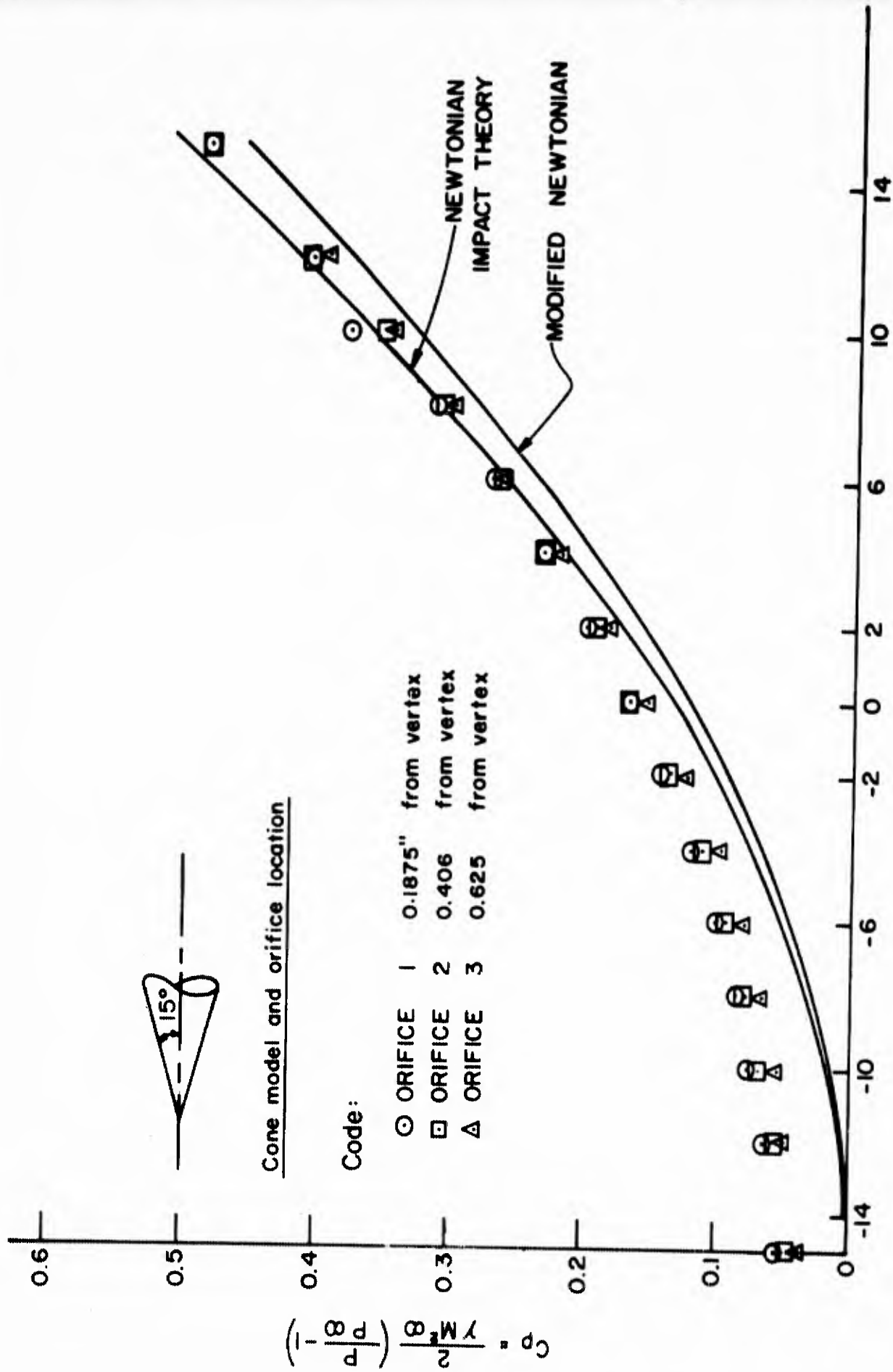


Figure 26. Pressure coefficient versus angle of attack for the 15° cone; $M = 10.95$; $Re = 3.58 \times 10^5$ per ft.

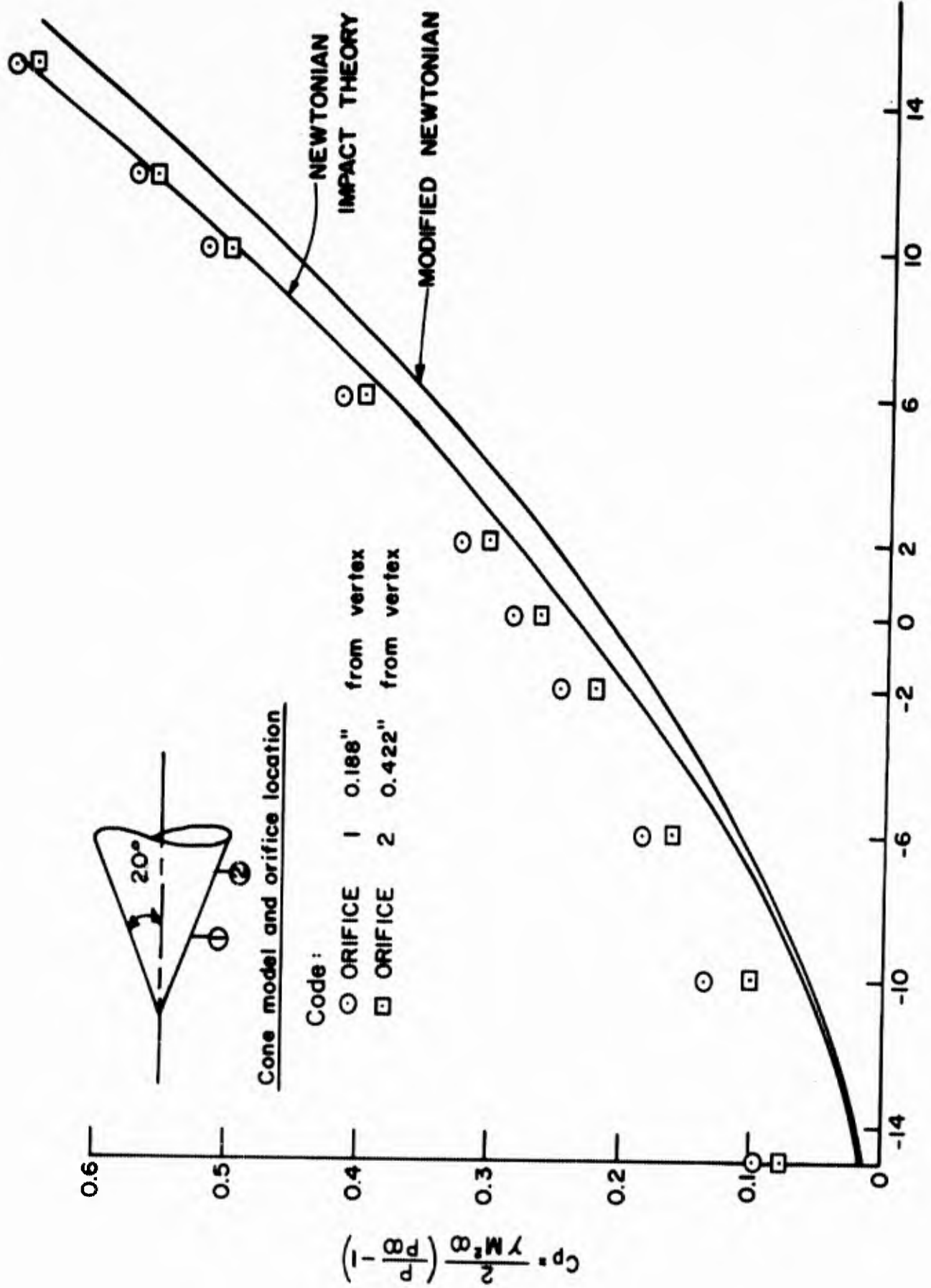


Figure 27. Pressure coefficient versus angle of attack for the 20° cone; M = 10.72; Re = 1.88 x 10⁵ per ft.

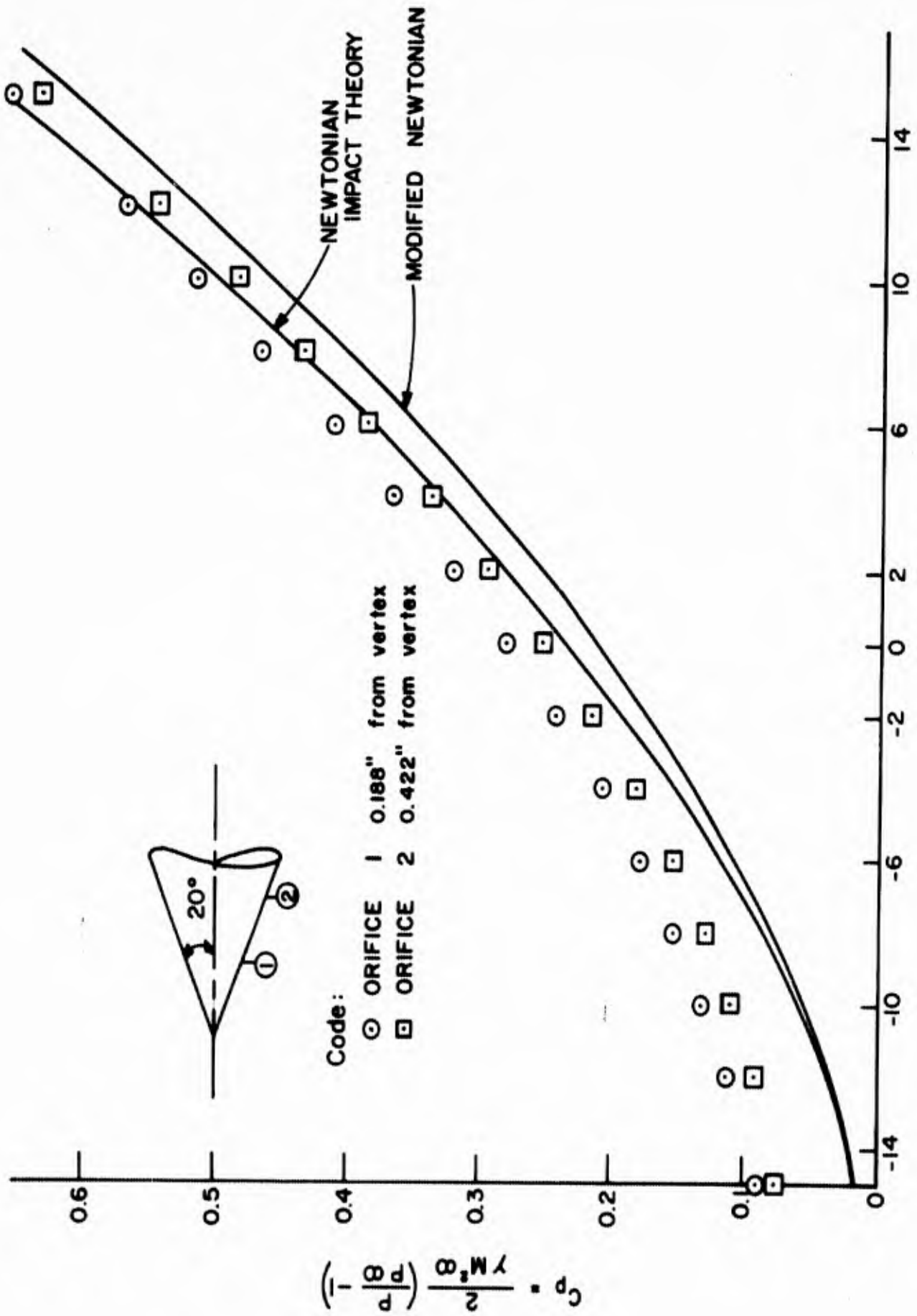


Figure 28. Pressure coefficient versus angle of attack for the 20° cone; M = 10.86; Re = 2.86 x 10⁵ per ft.

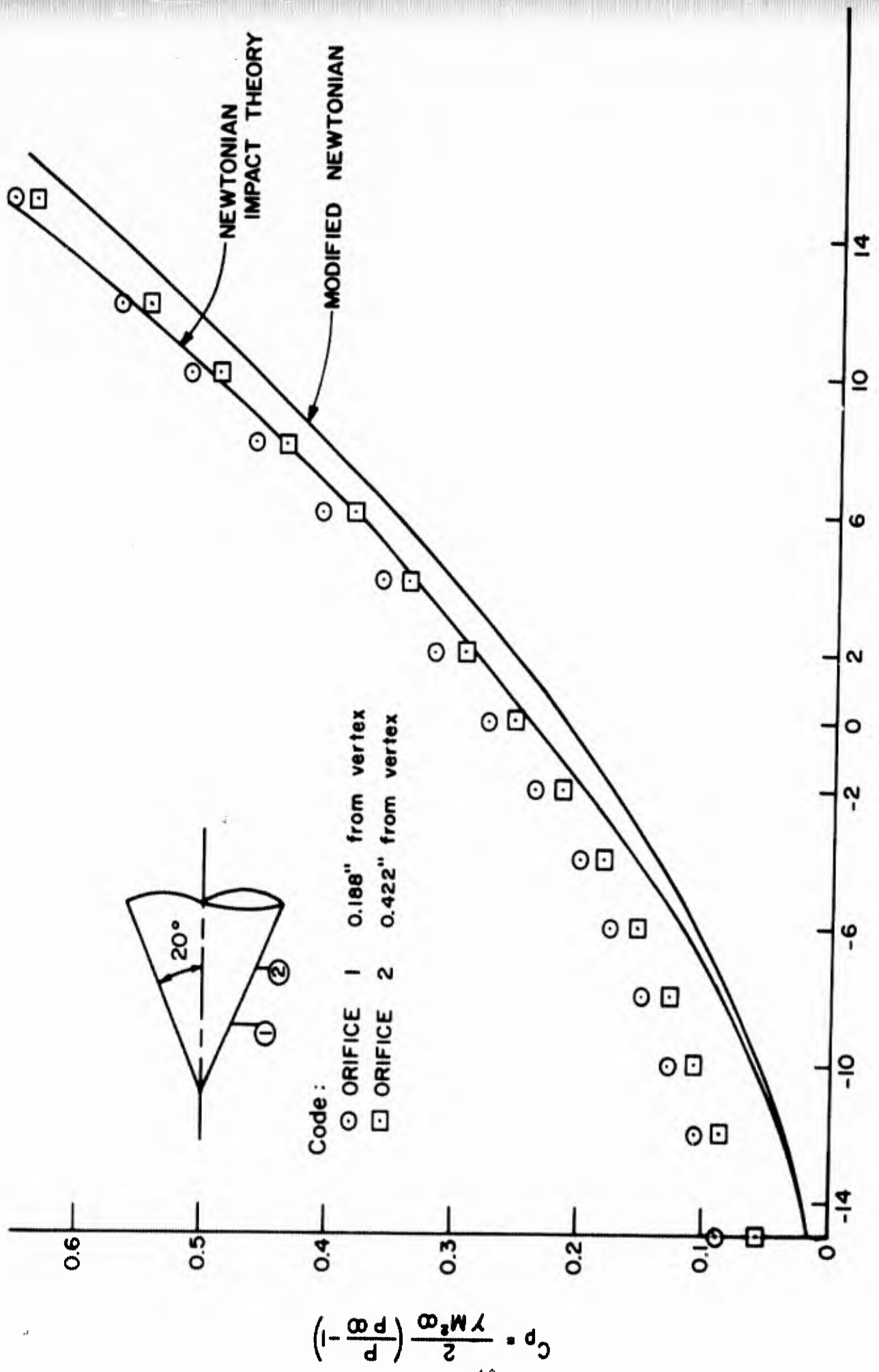


Figure 29. Pressure coefficient versus angle of attack for the 20° cone; $M = 10.95$; $Re = 3.58 \times 10^5$ per ft.

UNCLASSIFIED

UNCLASSIFIED

Aeronautical
Aeronautical Research Laboratories, Wright-
Patterson AFB, Ohio. HYPERSONIC VIS-
COUS FLOW OVER CONES AT NOMINAL
MACH 11 IN AIR by 1/Lt. John Anderson,
ARL. July 1962. 48 p. incl illus. (Project
7064; Task 7064-01) (ARL 62-387)

Aeronautical
Aeronautical Research Laboratories, Wright-
Patterson AFB, Ohio. HYPERSONIC VIS-
COUS FLOW OVER CONES AT NOMINAL
MACH 11 IN AIR by 1/Lt. John Anderson,
ARL. July 1962. 48 p. incl illus. (Project
7064; Task 7064-01) (ARL 62-387)

Unclassified Report

Unclassified Report

Experimental results were obtained on weak-
interaction, self-induced pressures on cones
at nominal Mach 11 in air using the ARL
3-inch continuous flow hypersonic wind tunnel.
The results at zero angle of attack were com-
pared with Probststein's first-order weak-

Experimental results were obtained on weak-
interaction, self-induced pressures on cones
at nominal Mach 11 in air using the ARL
3-inch continuous flow hypersonic wind tunnel.
The results at zero angle of attack were com-
pared with Probststein's first-order weak-

(over)

(over)

UNCLASSIFIED

UNCLASSIFIED

interaction theory and with Talbot's numeri-
cal method for predicting self-induced
pressures. Theory agreed well with the ex-
perimenta; data for 5-degree and 10-degree
semivertex angle cones, but over-estimated
the experimental induced pressures for 15-
degree and 20-degree cones. The results
were correlated reasonably well by the hyper-
sonic viscous-inter-action parameter and
the hypersonic similarity parameter. The
experimental results obtained for the 10-, 15-
and 20-degree cones at angles of attack from
-15 to 15 degrees compared favorably with
Newtonian theory for angles of attack greater
than 3 degrees. For values less than 3 degrees
degrees, Newtonian theory did not agree with
the experimental results.

interaction theory and with Talbot's numeri-
cal method for predicting self-induced
pressures. Theory agreed well with the ex-
perimenta; data for 5-degree and 10-degree
semivertex angle cones, but over-estimated
the experimental induced pressures for 15-
degree and 20-degree cones. The results
were correlated reasonably well by the hyper-
sonic viscous-inter-action parameter and
the hypersonic similarity parameter. The
experimental results obtained for the 10-, 15-
and 20-degree cones at angles of attack from
-15 to 15 degrees compared favorably with
Newtonian theory for angles of attack greater
than 3 degrees. For values less than 3 degrees
degrees, Newtonian theory did not agree with
the experimental results.

UNCLASSIFIED

UNCLASSIFIED

| | | |
|---------------------|---|---------------------|
| <p>UNCLASSIFIED</p> | <p>Aeronautical Aeronautical Research Laboratories, Wright-Patterson AFB, Ohio. HYPersonic VISCOUS FLOW OVER CONES AT NOMINAL MACH 11 IN AIR by 1/Lt. John Anderson, ARL. July 1962. 48 p. incl illus. (Project 7064; Task 7064-01) (ARL 62-387)</p> <p>Unclassified Report</p> <p>Experimental results were obtained on weak-interaction, self-induced pressures on cones at nominal Mach 11 in air using the ARL 3-inch continuous flow hypersonic wind tunnel. The results at zero angle of attack were compared with Probststein's first-order weak-</p> <p>(over)</p> | <p>UNCLASSIFIED</p> |
| <p>UNCLASSIFIED</p> | <p>interaction theory and with Talbot's numerical method for predicting self-induced pressures. Theory agreed well with the experimental data for 5-degree and 10-degree semivertex angle cones, but over-estimated the experimental induced pressures for 15-degree and 20-degree cones. The results were correlated reasonably well by the hypersonic viscous-interaction parameter and the hypersonic similarity parameter. The experimental results obtained for the 10-, 15- and 20-degree cones at angles of attack from -15 to 15 degrees compared favorably with Newtonian theory for angles of attack greater than 3 degrees. For values less than 3 degrees the experimental results.</p> <p>(over)</p> | <p>UNCLASSIFIED</p> |

| | | |
|--------------|--|--------------|
| UNCLASSIFIED | <p>Aeronautical Aeronautical Research Laboratories, Wright-Patterson AFB, Ohio. HYPERSONIC VISCOUS FLOW OVER CONES AT NOMINAL MACH 11 IN AIR by 1/Lt. John Anderson, ARL. July 1962. 48 p. incl illus. (Project 7064; Task 7064-01) (ARL 62-387)</p> <p>Unclassified Report</p> <p>Experimental results were obtained on weak-interaction, self-induced pressures on cones at nominal Mach 11 in air using the ARL 3-inch continuous flow hypersonic wind tunnel. The results at zero angle of attack were compared with Probstein's first-order weak-</p> <p>(over)</p> | UNCLASSIFIED |
| UNCLASSIFIED | <p>Aeronautical Aeronautical Research Laboratories, Wright-Patterson AFB, Ohio. HYPERSONIC VISCOUS FLOW OVER CONES AT NOMINAL MACH 11 IN AIR by 1/Lt. John Anderson, ARL. July 1962. 48 p. incl illus. (Project 7064; Task 7064-01) (ARL 62-387)</p> <p>Unclassified Report</p> <p>Experimental results were obtained on weak-interaction, self-induced pressures on cones at nominal Mach 11 in air using the ARL 3-inch continuous flow hypersonic wind tunnel. The results at zero angle of attack were compared with Probstein's first-order weak-</p> <p>(over)</p> | UNCLASSIFIED |

UNCLASSIFIED

UNCLASSIFIED

UNCLASSIFIED

UNCLASSIFIED

UNCLASSIFIED

UNCLASSIFIED

| | | |
|---|---|---|
| <p>Aeronautical Aeronautical Research Laboratories, Wright-Patterson AFB, Ohio. HYPERSONIC VISCOUS FLOW OVER CONES AT NOMINAL MACH 11 IN AIR by 1/Lt. John Anderson, ARL. July 1962. 48 p. incl illus. (Project 7064; Task 7064-01) (ARL 62-387)</p> <p style="text-align: center;">Unclassified Report</p> <p>Experimental results were obtained on weak-interaction, self-induced pressures on cones at nominal Mach 11 in air using the ARL 3-inch continuous flow hypersonic wind tunnel. The results at zero angle of attack were compared with Probststein's first-order weak-</p> <p style="text-align: center;">(over)</p> | <p>Aeronautical Aeronautical Research Laboratories, Wright-Patterson AFB, Ohio. HYPERSONIC VISCOUS FLOW OVER CONES AT NOMINAL MACH 11 IN AIR by 1/Lt. John Anderson, ARL. July 1962. 48 p. incl illus. (Project 7064; Task 7064-01) (ARL 62-387)</p> <p style="text-align: center;">Unclassified Report</p> <p>Experimental results were obtained on weak-interaction, self-induced pressures on cones at nominal Mach 11 in air using the ARL 3-inch continuous flow hypersonic wind tunnel. The results at zero angle of attack were compared with Probststein's first-order weak-</p> <p style="text-align: center;">(over)</p> | <p style="text-align: center;">UNCLASSIFIED</p> |
| <p style="text-align: center;">UNCLASSIFIED</p> <p>interaction theory and with Talbot's numerical method for predicting self-induced pressures. Theory agreed well with the experimental data for 5-degree and 10-degree semivertex angle cones, but over-estimated the experimental induced pressures for 15-degree and 20-degree cones. The results were correlated reasonably well by the hypersonic viscous-inter-action parameter and the hypersonic similarity parameter. The experimental results obtained for the 10-, 15- and 20-degree cones at angles of attack from -15 to 15 degrees compared favorably with Newtonian theory for angles of attack greater than 3 degrees. For values less than 3 degrees degrees, Newtonian theory did not agree with the experimental results.</p> <p style="text-align: center;">(over)</p> | <p style="text-align: center;">UNCLASSIFIED</p> <p>interaction theory and with Talbot's numerical method for predicting self-induced pressures. Theory agreed well with the experimental data for 5-degree and 10-degree semivertex angle cones, but over-estimated the experimental induced pressures for 15-degree and 20-degree cones. The results were correlated reasonably well by the hypersonic viscous-inter-action parameter and the hypersonic similarity parameter. The experimental results obtained for the 10-, 15- and 20-degree cones at angles of attack from -15 to 15 degrees compared favorably with Newtonian theory for angles of attack greater than 3 degrees. For values less than 3 degrees degrees, Newtonian theory did not agree with the experimental results.</p> <p style="text-align: center;">(over)</p> | <p style="text-align: center;">UNCLASSIFIED</p> |
| <p style="text-align: center;">UNCLASSIFIED</p> | <p style="text-align: center;">UNCLASSIFIED</p> | <p style="text-align: center;">UNCLASSIFIED</p> |

UNCLASSIFIED

UNCLASSIFIED